

Article

Improving the Energy Performance of a Household Using Solar Energy: A Case Study

Carmen Mârza, Raluca Moldovan ^{*}, Georgiana Corsiuc and Gelu Chisăliță

Faculty of Building Services Engineering, Technical University of Cluj-Napoca, 21 December 1989 Avenue 128-130 no., 400604 Cluj-Napoca, Romania; carmen.marza@insta.utcluj.ro (C.M.); georgiana.iacob@insta.utcluj.ro (G.C.); gelu.chisalita@insta.utcluj.ro (G.C.)

* Correspondence: raluca.moldovan@insta.utcluj.ro

Abstract: In the global context of energy transition from fossil fuels to renewable sources of energy, solar energy plays a key role in electricity generation, having the highest annual growth in the last years. This case study focuses on improving the overall energy efficiency of a household through thermal retrofitting, harnessing solar energy with photovoltaic (PV) systems and using air-source (ASHP) or ground-source (GSHP) heat pumps. The electricity generated by the PV systems is used to power the heat pumps and all other electricals of the household. The simulations for the ASHP and GSHP systems were conducted with GeoT*SOL software, while for electricity generation by PV systems, PV*SOL Premium software was used. The comparative results show: a decrease in the heating load to about 51.56%; an annual heating requirement of 53.88% of the normed one; an energy consumption index of about 58.34 kWh/m²·year; an annual energy consumption reduction of 88% for ASHP and 91% for GSHP, compared with the current gas heating system; 34% of the household consumption was covered by the PV system in the case of using ASHP and 36% for GSHP; and lower operating costs by 47% for the PV system with ASHP and 53% for the PV system with GSHP.

Keywords: solar energy; thermal retrofit; photovoltaic panel; heat pump; energy efficiency



Citation: Mârza, C.; Moldovan, R.; Corsiuc, G.; Chisăliță, G. Improving the Energy Performance of a Household Using Solar Energy: A Case Study. *Energies* **2023**, *16*, 6423. <https://doi.org/10.3390/en16186423>

Academic Editor: Carlo Renno

Received: 27 July 2023

Revised: 28 August 2023

Accepted: 2 September 2023

Published: 5 September 2023



Copyright: © 2023 by the authors. Licensee MDPI, Basel, Switzerland. This article is an open access article distributed under the terms and conditions of the Creative Commons Attribution (CC BY) license (<https://creativecommons.org/licenses/by/4.0/>).

1. Introduction

Two of the essential issues facing humanity and the planet at present concern energy resources and environmental conservation, which represent fundamental pillars within the concept of sustainable development.

The demographic, socio-economic and technological developments have led to a continuous increase in the world's energy demands. Based on information from Our World in Data, in 2021, the global primary energy consumption was more than 176,430 TWh, of which around 82% came from fossil fuels while approximately 13% from renewable sources [1]. Considering the limited nature of these resources, their dependency from other countries, their increasing price but especially the negative impact of their use on the environment and society due to the significant contribution to the increase in greenhouse gas (GHG) emissions, a global shift from fossil fuels to low-carbon sources of energy will be necessary [1,2]. The continuous development and improvement of technologies for the harnessing of renewable energy sources (RESs) represent a key factor in achieving this energy transition [3].

Worldwide, in the energy mix, the share of renewables in electricity generation grew fast, reaching 28.36% in 2021 and, among the renewable sources of energy, solar energy had the greatest annual growth of 22% from 2020 to 2021 and almost 24% from 2021 to 2022 [1].

Solar energy is the world's most important, abundant and available source of energy [4,5]. Solar energy is the Earth's energy source that allows life on Earth to be sustained and is part of the category of clean, non-polluting energies, contributing to the drastic reduction in substance emissions, especially of GHG emissions. It can be converted and

used as a resource for various technical applications, such as electricity generation, lighting, water heating and commercial or industrial consumption [6].

It is an inexhaustible source and is the result of the thermonuclear reactions of hydrogen transformation into helium that take place in the Sun, as a result of which a flow of radiant energy is continuously and constantly released into space [7] (pp. 17–19) [8]. More precisely, the Sun emits electromagnetic energy, with a rate of about 3.8×10^{23} kW/s. The Earth intercepts only a part of this amount, particularly, 1.8×10^{14} kW/s. Further, about 60% of this, which represents 1.08×10^{14} kW/s, reaches the surface of the Earth, with the other part being absorbed by the atmosphere or reflected back into space [9].

The radiations that reach the Earth are the following: ultraviolet radiation (3%), visible radiation (42%) and infrared radiation (55%). They have different wavelengths [10] (p. 11), as shown in Figure 1:

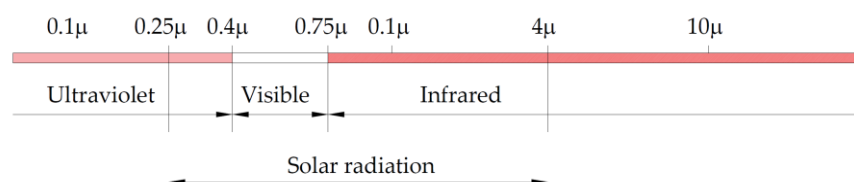


Figure 1. Solar radiation wavelengths.

One can see that a significant amount of solar energy is found in the field of infrared radiation and not in the field of visible radiation, which leads to the idea that this radiation can be efficiently captured, even in conditions where the sky is not perfectly clear.

The Sun can be considered an absolute black body, and the power emitted in a unit of time, per unit of surface, by an absolute black body depends only on its temperature [11] (pp. 65–69). It can be considered that the surface temperature of the absolute black body that emits the same amount of energy as the Sun is 5777 K, i.e., 5504 °C [11] (pp. 65–69) [12] (pp. 3–9).

The amount of energy that comes from the Sun and falls in a unit of time on a unit surface, perpendicular to the solar rays, at the outer limit of the terrestrial atmosphere (stratosphere) is called the solar constant E_0 (W/m^2). This value has undergone small corrections over time, mainly due to changes of the Sun–Earth distance [12] (pp. 3–9). Following the measurements made with the help of satellites, it can be approximated to a value of $1367 W/m^2$, also adopted by the World Radiation Center [13]. The flow of radiant energy that still reaches the Earth is diminished by the crossing of the terrestrial atmosphere, namely (7–17) km through the troposphere, to the value of about $900 W/m^2$.

The atmosphere modifies the intensity and spectral and spatial distribution of solar radiation through two mechanisms: absorption and diffusion.

The absorbed radiation is generally transformed into heat (air heat, water heat, latent heat of evaporation of seas and oceans water), and the diffused radiation is retransmitted in all directions into the atmosphere.

Global radiation is decomposed into direct, diffuse radiation and albedo, the latter representing the fraction of radiation diffused or reflected by the soil [14] (pp. 97–112).

The variation of solar radiation at the level of the Earth's surface depends on the following parameters [7] (pp. 17–19): the incidence angle of solar radiation (measured relative to the horizontal plane), the inclination angle of the Earth's axis, the Earth–Sun distance, geographic latitude and meteorological factors, including the transparency of the atmosphere, the cloudiness, the type of cloud formations and their thickness and position. The greatest impact is caused by cloudiness and the type of clouds (they even reduce by 90% the amount of solar radiation reaching the Earth's surface).

The most direct way of converting solar energy into a useful form of energy is obtaining electricity with the help of photovoltaic (PV) cells.

In 2022, the global cumulative capacity of solar PV energy reached around 1185 GW and reduced CO₂ emissions with almost 1399 MtCO₂eq, so as a result of the fast-growing

installing capacity, the decrease in the price of modules and the reduction in CO₂ emissions, solar PV technologies represent an essential contributor to the global energy transformation [15].

In the context of energy transition, among environmentally friendly technologies, PV panels and heat pumps (HPs) are known to have the most dynamic development [16]. As in the case of PV panels, heat pumps are widely recognized as an efficient technology for carbon emission reduction, as Rosenow et al. [17] highlighted, but also for the increase in energy efficiency and the promotion of renewable sources of energy. Harnessing the available energy from the air, water or ground and consuming electricity, heat pumps can provide thermal energy and, when the electricity need comes from low-carbon sources, the thermal energy delivered by HPs will be low or zero carbon [17].

As a result of energy independence from primary energy resources, HPs contribute to increasing the security of energy supply. Being more energy efficient than natural gas boilers, in the current context of the global energy crisis, HPs reduce the exposure of households to rising fossil fuel prices and significantly decrease greenhouse gas emissions [18]. According to the report from International Energy Agency (IEA 2022) [18], even though heat pumps in 2021 covered only about 10% of global heating requirements, the pace of their installation is growing rapidly. HPs are seen at present as the main means of decarbonizing the heating of many types of environments, estimating an increase in the overall capacity of heat pumps from 1000 GW in 2021 to almost 2600 GW by 2030.

Despite the higher cost of clean technologies, which will decrease in time, the total cost has to be analyzed over their lifetime and, based on an estimation made for 2030–2040 regarding the cost in EUR/kWh for different heating technologies, heat pumps and solar thermal are the ones with the lowest prices, being 68. . .76% cheaper than coal stoves and 51. . .63% cheaper than gas boilers [19].

Based on these data and the high prices for electricity and gas, using heat pumps powered by photovoltaic systems will reduce the dependency on fossil fuels and their rising prices, diminish consumers' energy bills and also contribute to reducing carbon emissions. In 2022, at the European Union level, both solar PV and heat pump technologies reached a record growth and, consistent with the report Solar Power Heat [20], solar PV installations rose by 47% compared with 2021, while heat pump installations grew by 42%.

Among heat pumps, ground-source heat pumps (GSHPs) are considered the most efficient technologies that are always subject to innovation in order to continuously improve the overall efficiency and, based on the significant contributions made by some researchers, it was concluded that, by coupling different auxiliary components (such as solar panels, boilers, cooling towers and lately dry coolers, in addition to improving the system's performance, the soil thermal storage is maintained in balance [21–23].

According to EU regulations [24,25], solar energy will be the key to achieving the goal of reducing dependence on fossil fuels, being able to supply a substantial part of the heat and electricity demand of a building by using photovoltaic systems and heat pumps. Additionally, the expansion of the use of heat pumps should be addressed in parallel with the increase in the number of installed solar PV systems, as the combination of them is considered to be the most energy-efficient solution [25].

In Romania, as result of the analysis sessions between the representatives of the European Commission DG Clima and representatives of the Romanian authorities, several objectives were established for the period of 2021–2030, among which one mentions measures to improve the energy efficiency, objectives related to reductions in GHG emissions by at least 40% compared to 1990 and objectives regarding the consumption of renewable sources. Related to the latter, it was established that the renewable energy target in 2030 should increase the level of ambition from 27.9% to 34% [26]. According to the 2021–2030 Integrated National Energy and Climate Plan for Romania, to reach the planned target, it is estimated that, for the years 2025 and 2030, an increase in the share of solar energy to 15% and almost 20%, respectively, of the gross final consumption of electricity from renewable sources is needed, while in the gross final consumption of electricity from re-

newable sources in the heating and cooling sector, heat pumps and solar thermal panels will represent viable alternatives [26].

In the Renovation Strategy Project on long-term building funds, in which the solutions are established based on a multi-criteria analysis, the proposed goal is to achieve energy class A for all types of buildings, except for single-family homes, where energy class B is accepted.

From the point of view of RES use, it is recommended to encourage the development of prosumers and the installation of photovoltaic panels, heat pumps and solar thermal panels. In this context, the Romanian government supports the deployment rooftop PV panels for residential buildings under the national net metering regime through the Green PV Home program. According to the latest statistics from the International Renewable Energy Agency, Romania had 1.39 GW of solar panels installed by the end of 2020 [27] and over 1.7 GW in 2022 [28]. It is estimated that, by 2030, the energy consumption from solar panels mounted on roofs will reach a value of 2.5 TWh, which represents 46.3% of the total increase in the production of electricity produced from solar panels [26].

In this paper, the authors propose solutions to improve the energy performance of a household, aimed towards:

- ✓ The thermal rehabilitation of the building envelope;
- ✓ The addition of PV panels for the production of electricity; thus, the current case based on measurements and the one proposed by simulation are presented;
- ✓ The use of heat pumps for heating, replacing the current situation in which a gas plant is used.

2. Materials and Methods

The goal of this study was to save energy and to lower operating costs for a single-family home in Romania, first by thermal insulation using energy-efficient and environment friendly materials and then by harnessing solar energy through photovoltaic panels and heat pumps. The schematic design of the proposed solutions is shown in Figure 2.

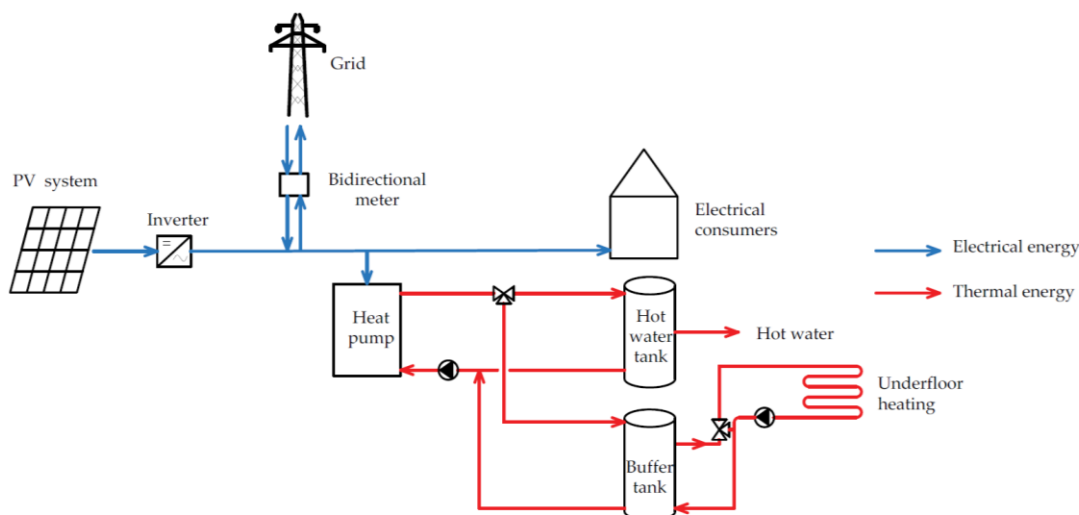


Figure 2. Schematic design of the heat pump and PV system.

To assess the impact of the proposed solutions compared to the current situation, various tools and software were used. The analysis started from the gas and electricity consumption recorded for the studied period, namely, the year 2022.

To simulate the energy production of the proposed PV system, two programs were used, namely, PVGIS and PV*SOL Premium.

The PVGIS program [29] provides information about solar radiation and the electricity production of photovoltaic systems for various panel-mounting positions in any location in Europe.

PV*SOL Premium [30] is a design and simulation software for PV systems with the 3D visualization of the building and panel assembly, as well as the analysis of factors that influence system performance, such as shading analysis.

Regarding the thermal analysis of the building, the determination of the main characteristics of the building elements, the calculation of the heating demand for heating and domestic hot water and the analysis of the annual energy requirements, the current technical standards and norms were used [31–36]. For this purpose, Microsoft Excel[®] software was used, by creating workbooks containing custom spreadsheets, which allowed us to obtain the numerical and graphical results presented below in this paper.

The simulations for the heat pump systems were made using GeoT*SOL software, a professional tool for the design and calculation of heat pump systems [37]. Considering climate data for different locations, databases for different types of systems and components, various heat sources and modes of operation, the heat pump systems can be simulated, determining the energy generated, electricity consumption (from yearly to hourly scale) and seasonal performance factor (SPF) [37,38].

2.1. Case Study and Solar Energy Context in Romania/Aiud

In Romania, five different geographical areas were identified according to the level of recorded energy flow, as it is shown in Figure 3 [39]. The geographical distribution regime of the solar energy potential shows that more than half of the country's surface benefits from an average annual solar irradiation of 1200 kWh/m².

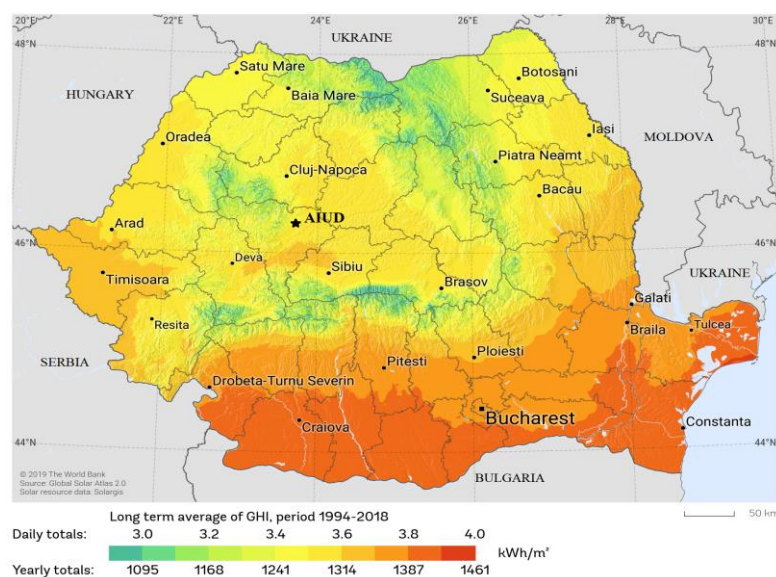


Figure 3. Photovoltaic potential of Romania [39].

The house for which the study was conducted, in order to improve its energy performance, is situated in Aiud-Alba County and was built in 1998. It has a building footprint of 144 m² with a basement and 2 stories (Figure 4). The height of the stories is 2.50 m. The roof of the house has two sides with an E–W orientation, having an 35° inclination. At that time, at least in our country, there was no special emphasis on the energy performance of buildings both due to the lack of appropriate materials and technologies as well as the mentality of the people, who did not realize the need for a special respect for energy consumption and the environment.

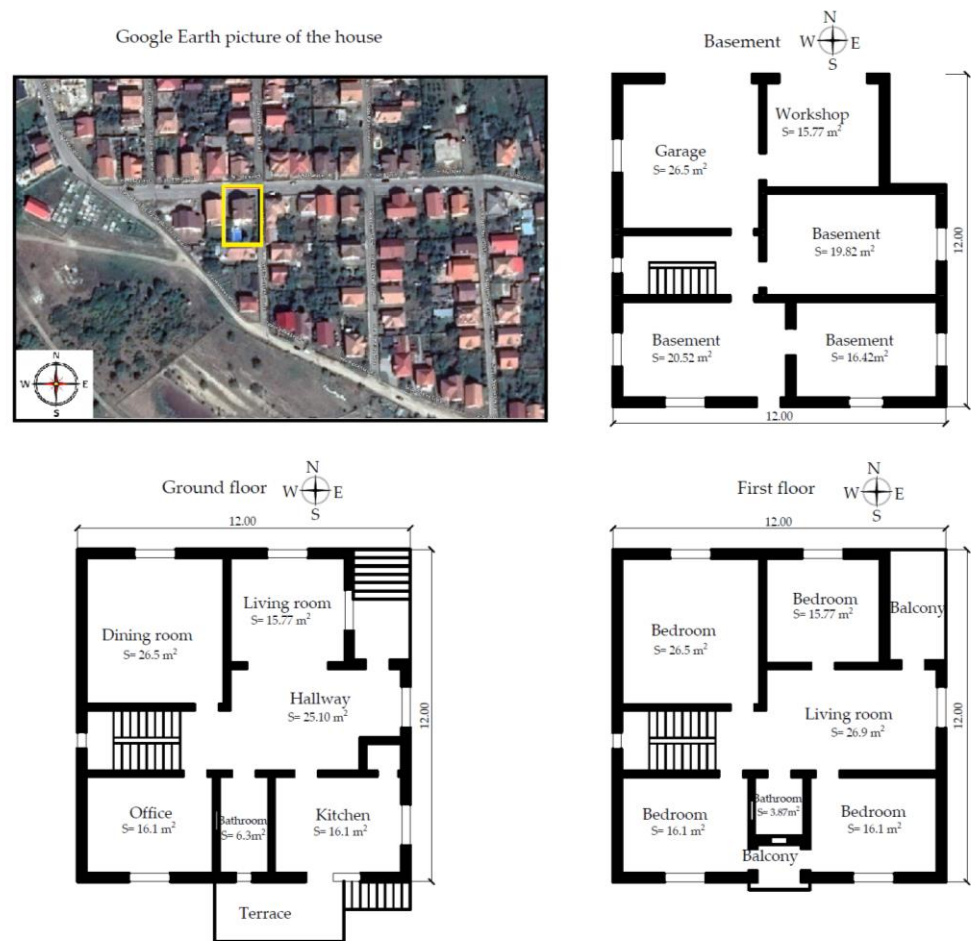


Figure 4. Case study house: Google Earth picture and floor plans of the house.

The level of solar radiation is one of the essential factors that influence the performance of the photovoltaic system. The PVGIS program allows access to information about hourly, daily or monthly values of solar radiation. Thus, Figure 5 shows the monthly values of solar radiation for the location of the studied house. The panels respect the slope of the roof, respectively 35°.

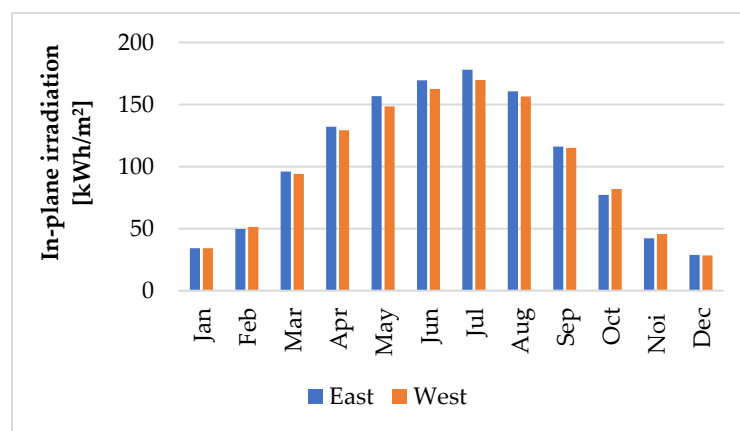


Figure 5. Monthly in-plane irradiation for a fixed angle.

Figures 6 and 7 show the average values of solar radiation during one day in the months of July and December for the two sides of the roof, respectively the months with the highest and the lowest values of solar radiation.

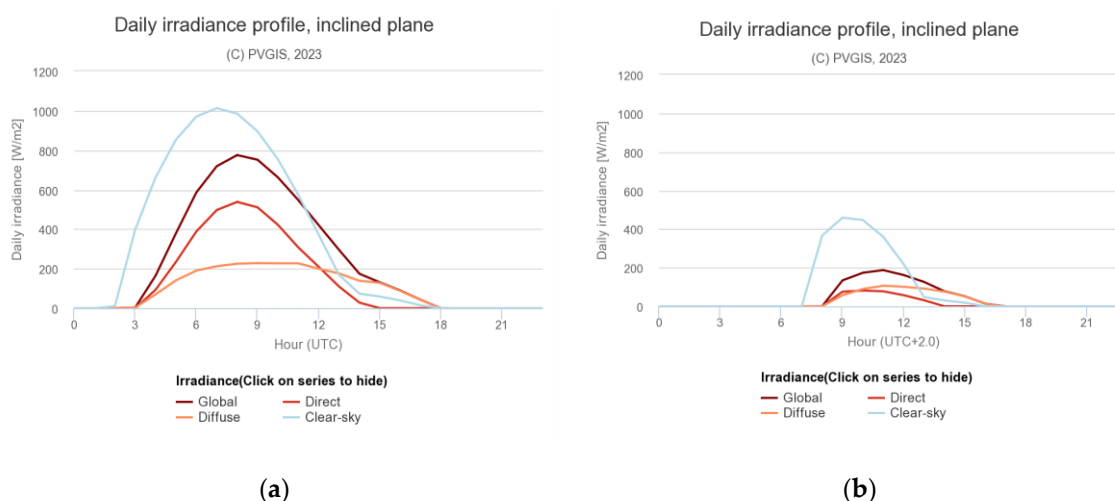


Figure 6. Daily average irradiance on a fixed plane with a slope of 35° and azimuth of -90° (East). (a) July. (b) December.

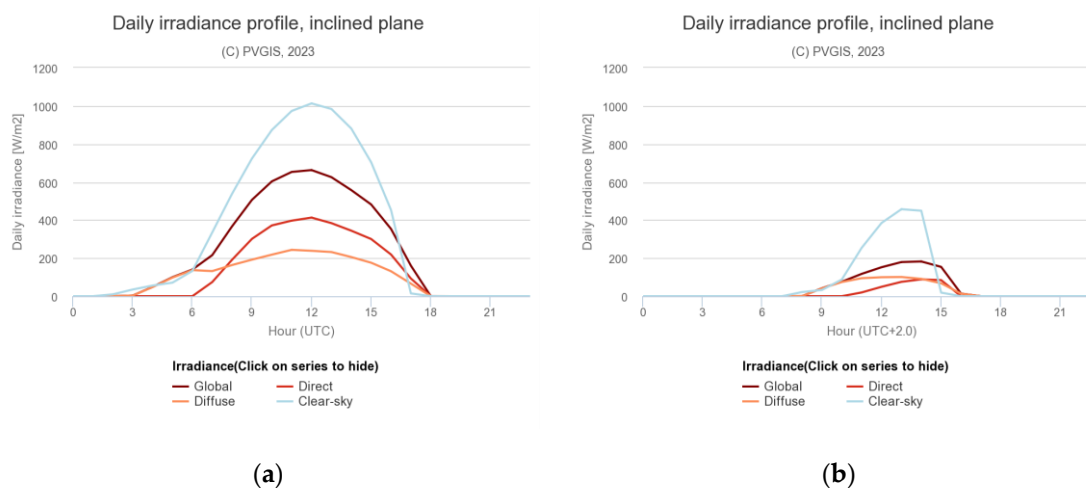


Figure 7. Daily average irradiance on a fixed plane with a slope of 35° and azimuth of 90° (West). (a) July. (b) December.

2.2. Current Structures of Building Elements

2.2.1. Main Building Elements

In order to make proposals for improving the structure of the building elements under study, an extensive analysis of the current situation regarding geometric, physical and thermal characteristics was conducted.

The construction elements of the building were divided into the following main categories: exterior walls (reinforced concrete, autoclaved aerated concrete or AAC and brick), interior walls (brick masonry and AAC), slab floors with parquet or tiles as the finishing layer and a slab floor over the last level and roof. Regarding the glazed construction elements, the windows, exterior doors and interior doors were taken into account.

Using the values of the thermophysical properties of the building materials and the indicated surface heat transfer coefficients, the following important characteristics of the studied building elements were determined: thermal inertia index D , thermal massiveness coefficient m , thermal resistance R and the overall heat transfer coefficient k or U -value.

The thermal inertia index D , the thermal assimilation coefficient s and the coefficient of thermal massiveness m were determined using correlations from references [31,32] and the material properties tables, e.g., Annex A [31] or Annex 2.1 [32].

The specific thermal resistance R_s is usually calculated by using Formula (1) [31,32]:

$$R_s = \frac{\delta}{\lambda} \quad (1)$$

or its equivalent in English academic and technical literature (2):

$$R_s = \frac{L}{k} \quad (2)$$

where δ (or L for English)—layer thickness (m); and λ (or k for English)—thermal conductivity of the material ($W/m \cdot K$).

The thermal resistance R (the R-value) can be calculated by Formula (3), using the sum of the resistances R_j of all layers and the inside and outside air-film resistances [40,41]:

$$R = R_{si} + \sum_{j=1}^n R_j + R_{se} \quad (3)$$

where R_{si} —inside air-film resistance ($m^2 \cdot K/W$); $\sum_{j=1}^n R_j$ —sum of the resistances of “ n ” layers ($m^2 \cdot K/W$); and R_{se} —outside air-film resistance ($m^2 \cdot K/W$). The R-value unit of measurement in S.I. (International System of Units) for the specific thermal resistance is ($m^2 \cdot K/W$) and for absolute (total) thermal resistance is (K/W).

The Overall Heat Transfer Coefficient (OHTC) k or U-value is calculated using Formula (4) [31,32,42]:

$$k \equiv U = \frac{1}{R} \quad (4)$$

where R —thermal resistance (R-value) ($m^2 \cdot K/W$). The S.I unit for OHTC or U-value is ($W/m^2 \cdot K$).

2.2.2. Building Thermal Insulation

Among the main characteristics of the materials used for thermal insulation and the structures of thermally insulated building elements in general, there are the following: thermal conductivity λ (or k), thermal resistance, thermal transmittance thermal conductance etc. [42].

As we know, the thermal conductivity of a material represents the time rate of the steady state heat flow expressed in (W), through an area $A = 1 \text{ m}^2$ of thickness $L = 1 \text{ m}$ of a homogeneous material, in a direction perpendicular to isothermal plates, which is induced by a temperature difference $\Delta T = 1 \text{ K}$ across the sample [40,41]. Thermal conductivity, denoted by λ (or k in English), has the unit of ($W/m \cdot K$) in S.I. and generally is a function of material mean temperature and of the moisture content, material porosity pressure etc.. Basically, the thermal conductivity is a measure of how a material is efficient (or not) in conducting heat.

On the other hand, the thermal resistance (known as the R-value) represents a measure of the resistance or obstruction of heat flow as a result of diminishing the thermal conduction, the thermal convection and/or the thermal radiation [42]. Usually, the thermal resistance is considered to be a function of thermal conductivity, the thickness of material, density and some others practical factors, such as the subsidence occurred during exploitation.

Very important for the calculation of heating or cooling loads is the thermal transmittance, which is the rate of heat flow through an area $A = 1 \text{ m}^2$ of a structural element having a temperature difference $\Delta T = 1 \text{ K}$ between the surfaces of the two sides [41]. The thermal transmittance is also called the overall heat transfer coefficient and is denoted by k or the equivalent U-value in English.

Some of the most important factors that impact the proper selection of insulating materials are well summarized in [42] as follows:

- Thermal performance: thermal resistance, thermal bridging and thermal storage;
- Cost: cost of insulation, cost of materials and workmanship, and impact on labor cost;

- Ease of construction: impact on workmanship requirements, speed of construction, maintenance and replacement;
- Building codes' requirements: fire resistance, health hazards and structural stability;
- Durability: R-value changes over time, water and moisture effects, and dimensional stability;
- Acoustical performance: sound absorption and insulation;
- Air tightness: vapor or infiltration barrier and wall and roof construction quality;
- Environmental impact and availability.

It is worth noting that, when considering energy conservation issues and generally speaking thermal performance, one of the most important properties that is of interest is obviously the thermal resistance of insulation materials [42].

The following materials and composites are used for many types of building thermal insulation [41–43]:

- Inorganic materials: fibrous materials (slag wool, rock and glass) and cellular materials (perlite, vermiculite and calcium silicate);
- Organic materials: fibrous materials (cotton, wood, cane and cellulose) and cellular materials (polystyrene, polyurethane, foamed rubber and cork);
- Metallic/metallized reflective membranes with a gas-filled, air-filled or vacuous space.

Natural fibrous materials have numerous advantages over other materials and, being environmentally friendly and renewable materials, they are considered to be some of the most promising materials for building thermal insulation [43].

More recently, Kumar et al. [44] categorized building insulation materials using primarily three main types, based on their origin, chemical substance and availability:

1. Conventional: inorganic insulation materials (fibrous insulation materials and cellular insulation materials) and organic insulation materials (fibrous and cellular);
2. State of the art: closed-cell foam, aerogel [45], transparent insulation materials (TIM), vacuum insulation panels (VIP) [46], reflective multi-foiled insulation materials (RM-FIM), nano-insulation materials (NIM) and dynamic insulation materials (DIM);
3. Sustainable: bio-insulation materials (natural insulation materials based on agro- and forest-residues natural insulation materials based on sheep wool) and recycled insulation materials.

Amongst the three insulation types mentioned above, sustainable insulation materials have the lowest environmental impact during the production stage and also a lower embodied energy (EE) and embodied carbon (EC) [44].

Having proper physical characteristics, such as hygrothermal, fire resistance, strength, acoustic, naturally regulating the indoor environment, low embodied energy and low embodied carbon, make sheep wool a very good choice for a sustainable building insulation material [44,47]. Investigations conducted by Ye et al. [48] showed that hemp and sheep wool have an equal value of thermal conductivity at a given density, and Zach et al. [49] found that sheep wool, because of having hygroscopicity of up to 30%, can absorb a large amount of water vapor without significantly increasing its thermal conductivity.

Sheep wool can hold humidity by absorption up to 20% with a slight variation in thermal conductivity, at a temperature $t = 23\text{ }^{\circ}\text{C}$ and relative humidity range of $\text{RH} = 30. \dots 60\%$ [44].

A series of important characteristic properties of some natural building insulation materials, such as: corn, hemp, cotton stalk fibers, wood fibers and sheep wool, are shown in Table 1 (after [44]).

Table 1. Properties of some natural building insulation materials.

Insulation Type	Thermal Conductivity λ (or k) (W/m·K)	Density ρ (kg/m ³)	Specific Heat Capacity c_p (J/kg·K)	Embodied Energy EE (kJ/kg)	Embodied Carbon EC (kg CO ₂ /kg)	Ref.
Corn	0.101...0.139	148...257	1480...1720	–	–	[50]
Hemp	0.039...0.123	25...100	1700...1800	18,710	0.14	[51,52]
Cotton stalk fibers	0.058...0.082	150...450	130	44,000...480,000	2.40...2.70	[43]
Wood fiber	0.038...0.050	50...270	1900...2100	20,300	0.124	[53]
Sheep wool	0.038...0.054	10...20	1300...1700	5400	0.120	[54,55]

2.2.3. Glazed Building Elements

Glazed building elements (exterior fenestration and doors, glazed walls and skylights) have several roles, of which the most important are the following: obtaining natural lighting of rooms, the natural ventilation of interior spaces and to allow the partial passage of solar radiation [32].

The exterior fenestration and doors consist of frame (frame and sash) and glass panels. The frames are generally made of wood, metal or plastic (PVC and polyurethane) [31], and regarding their opening mode, they are single, double or coupled. Windows can be single (clear, absorbent or reflective) or thermally insulating (double or triple) [32].

Thermally insulating windows are usually made using two or three sheets of glass, welded or sealed on the contour, having between them a hermetically sealed space, filled with air or various inert gases: argon, krypton or xenon. One or both surfaces can be specially treated in order to significantly reduce heat loss by reducing the OHTC. Another manufacturing option is the use of three specially treated sheets of glass, between which there is a vacuum space with a very small size (about 0.13 mm) and a high thermal resistance [56].

Typically, the thickness of the glass pane is 4 mm, and the thicknesses of the gas layers can be 6, 9, 12, 15 or 20 mm. Thus, various configurations can be obtained, for example, 4-6-4 or 4-20-4 (double glazing with a gas layer of 6 mm or 20 mm) or 4-6-4-6-4 or 4-12-4-12-4 (triple glazing with two gas layers of 6 mm or 12 mm).

The OHTC or U-value for a single window (U_F), without or with additionally opaque panels, and the U-value for a fully glazed door (U_U) can be calculated using the correlations suggested in [31].

For example, the OHTC or U-value for a double- or triple-insulating glass (U_g), where the space between the glass sheets is filled with air, can be determined using Equation (5) [31]:

$$U_g = \frac{1}{R_{si} + \sum_{j=1}^{n_g} \frac{\delta_j}{\lambda_j} + \sum_{k=1}^{n_a} R_{a,k} + R_{se}} \quad (5)$$

where R_{si} —inside air-film resistance (m²-K/W); δ_j —the thickness of the glass panel or material layer “j” (m); λ_j —thermal conductivity of the glazing panel or material layer “j” (W/m K); $R_{a,j}$ —thermal resistance of the air layer “j” between the glazing sheets (m²-K/W); R_{se} —outside air-film resistance (m²-K/W); and n_g , n_a —number of glass panels air layers of the insulating window (–).

A series of U_g -values for double- and triple-insulating glasses, where the space between the glass sheets is filled with air, argon and krypton, for two typical configurations 4-6-4 and 4-20-4 (double glazing) and 4-6-4-6-4 and 4-12-4-12-4 (triple glazing), is presented in Table 2 (after [31]).

The values in Table 2 are valid for gases (argon or krypton) with a concentration greater than 90%. Inside and outside air-film resistances, R_{si} and R_{se} , respectively, were

considered with the following values: $R_{si} = \frac{1}{8} = 0.125 \frac{m^2 \cdot K}{W}$ and $R_{se} = \frac{1}{24} = 0.042 \frac{m^2 \cdot K}{W}$. For the thermal conductivity of glass, the value $\lambda = 1.0 \text{ W/m} \cdot \text{K}$ was used.

Table 2. The U_g -values for double- and triple-insulating glasses, with the space between the glass sheets filled with air, argon and krypton.

No.	Type	Windows	Coef. of Emission (-)	Dimensions (mm)	Air	Argon	Krypton	
1	Double-insulating glass	Normal glass untreated	0.89	4-6-4	3.3	3.0	2.8	
				4-20-4	2.7	2.6	2.6	
		One surface treated	≤ 0.40	4-6-4	2.9	2.6	2.2	
				4-20-4	2.2	2.0	2.0	
				4-6-4	≤ 0.10	2.6	2.2	1.7
						4-20-4	1.6	1.4
				4-6-4	≤ 0.05	2.5	2.1	1.5
						4-20-4	1.5	1.2
2	Triple-insulating glass	Normal glass untreated	0.89	4-6-4-6-4	2.3	2.1	1.8	
				4-12-4-12-4	1.9	1.8	1.6	
		One surface treated	≤ 0.40	4-6-4-6-4	2.0	1.7	1.4	
				4-12-4-12-4	1.5	1.3	1.1	
				4-6-4-6-4	1.70	1.3	1.0	
				4-12-4-12-4	≤ 0.10	1.1	0.9	0.6
						4-6-4-6-4	1.6	1.3
				4-12-4-12-4	< 0.05	1.0	0.8	0.5

For insulating windows with metal spacers, the linear heat transfer coefficient Ψ_g is indicated in Table 3, according to [31].

Table 3. Linear heat transfer coefficient Ψ_g for insulating windows with metal spacers.

No.	Type of Carpentry	Double and Triple Glazing; Untreated Windows (Air or Gas)	Double Glazing with a Treated Surface; Triple Glazing with Two Treated Surfaces (Air or Gas)
1	Wood and PVC	0.04	0.06
2	Metal	0.06	0.08
	Without interruption of thermal bridges	0.0	0.02

High quality windows and doors are currently a very important requirement for energy-efficient buildings. In order to obtain an OHTC value lower than $0.85 \text{ W/m}^2 \cdot \text{K}$ for the so-called “warm windows”, a proper installation is first necessary.

2.3. Heating Demand for Heating and Domestic Hot Water

The heating demand for heating a room is calculated using Formula (6) [32,33]:

$$Q = Q_T \cdot \left(1 + \frac{A_c + A_o}{100} \right) + Q_i \quad (6)$$

where Q_T —heat transfer rate (heat flow per unit time) yielded by transmission (W); Q_i —heat transfer rate required for heating the infiltrated air through the leaks of doors and

windows and also the air penetrated when opening them (W); A_c —add-on coefficient for compensating the effect of cold surfaces (–); A_o —cardinal orientation add-on coefficient (–).

The heat transfer rate Q_T yielded by transmission (including the heat transfer rate Q_s yielded through the soil) and the heat transfer rate Q_i required for heating the infiltrated air are calculated by using the appropriated correlations indicated in [33].

The annual energy (heat) demand for heating, per 1 m³ of internal volume, is determined by Formula (7) [35]:

$$Q = \frac{24}{1000} \cdot C \cdot N_{12}^{0_i} \cdot G - (Q_i + Q_s) \left[\frac{\text{kWh}}{\text{m}^3 \cdot \text{year}} \right] \quad (7)$$

where Q —annual energy (heat) demand for heating, per m³ of heated volume (kWh/m³·year); C —correction coefficient (–); $N_{12}^{0_i}$ —annual number of degrees–days taken into account (K·days); G —overall coefficient of the thermal insulation of the building (W/m³·K); Q_i —useful energy (heat) input from inhabiting the building, per 1 m³ of heated volume (kWh/m³·year); Q_s —useful energy (heat) input from solar radiation, per 1 m³ of heated volume (kWh/m³·year).

The annual number of degree–days taken into account $N_{12}^{0_i}$, the overall coefficient G of thermal insulation of the building and the useful energy (heat) input Q_s from solar radiation were calculated by formulae indicated in [35]. The useful energy (heat) input from inhabiting the building can be considered according to [35], with the value $Q_i = 7$ kWh/m³·year in the case of a residential building.

Particularly relevant in the current context, especially for low-energy buildings or energy-efficient buildings and passive houses, is to report the annual energy (heat) demand per m² of useful area. Using a set of relationships suggested in [35], we have:

$$Q_{1\text{m}^2} = 3.125 \cdot Q \left[\frac{\text{kWh}}{\text{m}^2 \cdot \text{year}} \right] \quad (8)$$

The thermal load (heating demand) for the preparation of domestic hot water (DHW), in the case of using a technical solution with storage, e.g., the use of DHW cylinders/storage tanks (also known in our technical literature as “boilers”), can be determined with the general correlation (9):

$$Q_{\text{DHW}} = \frac{n_p \cdot C_{zn} \cdot \rho \cdot c_p \cdot (t_B - t_{ar})}{3600 \cdot \tau} [\text{W}] \quad (9)$$

where n_p —number of persons (–); C_{zn} —DHW demand per person and day (L/pers·day); ρ —water density (kg/m³); c_p —specific heat of water (J/kg·K); t_B —DHW temperature in the DHW cylinder (°C); t_{ar} —average temperature of the supply (cold water) (°C); τ —DHW preparation time (h).

The volume of DHW cylinder is usually determined using Formula (10):

$$V_B = f \cdot V_{B,\text{min}} = f \cdot \frac{n_p \cdot C_{zn} \cdot (t_{\text{DHW}} - t_{ar})}{(t_B - t_{ar})} [\text{l}] \quad (10)$$

where f —oversizing factor (–); $V_{B,\text{min}}$ —minimum DHW cylinder volume (l); t_{DHW} —DHW supply temperature (°C); and n_p , C_{zn} , t_B , t_{ar} —the same as above.

The oversizing factor f has the value $f = 1$ in the case of using classical fuels, biogas, biomass or electricity and the value $f = 1.5 \dots 2$ for DHW preparation using solar energy and/or heat pumps.

2.4. Heat Pumps

Given the ability of the soil to store solar energy, both air- and ground-source heat pumps capitalize on solar energy, the former directly, the latter indirectly.

Due to the lower price of the investment and the simplicity in assembly, air-source heat pumps (ASHP) have the largest market share of heat pumps. However, the performance of these systems depends on the external climatic conditions, especially in cold areas [57]. As for ground-source heat pumps (GSHP), although they represent more efficient solutions (even in the case of the existing heating systems, with higher temperatures), in the markets of most EU states, they only hold a small market share compared to air-source heat pumps [58].

To cover the thermal energy demand for the building proposed for thermal retrofit, a heat pump was chosen and, to improve energy efficiency, to reduce carbon emissions and the operational cost of the heat pump [59], two scenarios were analyzed: a PV system and ASHP (case 1) and a PV system and GSHP (case 2).

The heat pump systems were designed to provide space heating and domestic hot water preparation for the proposed renovated house located in Aiud, Romania.

The simulations for the heat pump systems were conducted with the GeoT*SOL software [37], over a year. Two heat pump systems (HPSs) for space heating and DHW with buffer tank and DHW tank were selected, one with air source and the second one with ground source and geothermal collectors, due to the available land area. So, the simulations started from the annual heating requirements for heating and domestic hot water preparation and the following input data: climate data for Aiud, Romania; standard outdoor temperature of $-18\text{ }^{\circ}\text{C}$; low temperature for space heating ($35/30\text{ }^{\circ}\text{C}$); and monovalent mode of operation for GSHP and monoenergetic partially parallel for ASHP.

The selected heat pumps from the software have the following properties: the ASHP is a standard air/water heat pump with a nominal heating power of 13 kW and a heating element of 6 kW, 4.1 kW electrical power and a coefficient of performance (COP) of 3.2 for the standard temperatures (A2/W35) according to EN 14511; the GSHP is a standard brine/water heat pump with a nominal heating power of 14 kW, 3.26 kW electrical power and a COP of 4.3 for the standard temperatures (B0/W35) according to EN 14511, COP representing the ratio between the nominal heating power of the HP and the electrical power input for specific conditions.

Two scenarios were analyzed in comparison with the existing system based on heating with natural gas (case 0). The relevant performance values of the HP system, over a year, resulted from the simulation are seasonal performance factor and energies: energy generated by heat pump systems, energy used for heating and DHW and power consumptions for heat pump, heating element and auxiliary energy (fans and external pumps on the side of the heat source of the HP). The SPF of the HP is determined by simulation (in accordance with EN 15316-4-2 Heating systems in buildings—method for calculation of system energy requirements and system efficiencies—part 4-2: heat generation for indoor heating and heat pump systems). It represents the ratio between the heat supplied by the HP for heating and DHW and the power consumption of the HP (the compressor). For the HP system, SPF is expressed as the heat supplied by the HP and the heating element divided by the total electricity consumption of the HP, heating element and auxiliary energy.

The electricity generated by the PV system is used to power the heat pump systems and, when the PV system is only able to partially cover the electricity required for the heat pump systems, the rest is taken from the national electricity grid.

2.5. PV Panels

The most used material for the construction of PV cells is silicon, a cheap and abundant material on Earth. The silicon atom is tetravalent, meaning the four electrons in the outer orbit can be donated, shared or accepted by other atoms, being called valence electrons, with an important role in photovoltaic conversion. Through them, several atoms unite forming a crystal. Through the regular grouping of several crystals, a crystalline network is formed.

Depending on the composition of the material, one can have: monocrystalline silicon, polycrystalline silicon and amorphous silicon (similar to glass).

The PV panels on which the measurements and studies were made in this paper were of monocrystalline silicon, which is why certain specifications are provided.

A monocrystalline panel is obtained from a single silicon crystal by sectioning into thin slices a large and chemically pure vein [60] (pp. 118–120). Due to this execution technology, it is the most efficient type of cell in terms of conversion into electrical energy. Obviously, the costs are higher, but if a few years ago, there was a reason why polycrystalline ones were used, at present, the price difference has decreased, so that, weighing the advantages and disadvantages, monocrystalline ones have become preferred.

Currently, monocrystalline panels have an efficiency of about 22.5%, and according to studies, it seems that the maximum theoretical efficiency of conversion from light energy into electrical energy is 29% [61] (pp. 82–86).

An important role in obtaining an optimal degree of solar energy conversion comes from the orientation of the solar collectors. Their position is defined by two angles [7] (pp. 17–19):

- The angle of inclination, that is, the angle between the panel and the horizontal plane, which in the case of mounting on framework roofs, usually, is equal to the angle given by the inclination of the slopes;
- The azimuth angle represents the orientation of the receiver plane relative to the south direction.

Regarding the optimal tilt angle (OTP), several studies have been conducted on its value, so as to result in a maximum efficiency of solar radiation conversion (SRC). The results of Abdelaal et al. [62] showed that the optimal daily angle produces the highest value of SRC, but this is difficult and with high costs to apply in practice. Following some measurements and simulations made by the authors, it turned out that the alternation of two inclinations provides good results in the warm season and in the cold season, being lower by only 1.56% than in the case of daily adjustment.

As is known in the technical literature, the optimal angle of inclination is approximately equal to the latitude. For the northern hemisphere, in autumn and winter, the recommended angle of inclination is given by the latitude of the location $+15^\circ$, so that the PV panel is positioned towards the Sun, which in winter has a lower height. In the summer, the situation being reversed, the angle of inclination is lower, and it is recommended to be equal to the latitude -15° [7,62].

Another factor that negatively influences the operation of a photovoltaic system is represented by shading. This can be due to tall buildings in the neighboring areas, the vegetation in the area or architectural elements in the structure of the building itself. In this latter case, the analyzed building was included. The roof with two sides with E–W orientation has an awning on both slopes, which produces shading on certain areas, obviously depending on the position of the Sun.

The partial shading that involves the unequal distribution of light intensity can generate the appearance of hot-spot points on the PV modules, which has negative effects on the performance and integrity of the modules [63].

In 2021, the owners of the assessed house installed 8 monocrystalline photovoltaic panels through the Green PV Home Program, each having an efficiency of 19.6% and a power of 395 W, yielding an installed power of 3.16 kW.

As can be seen in Figure 8, four panels were installed on the eastern slope and four panels on the western slope.



Figure 8. The position of the PV panels (existing situation).

The chart in Figure 9 shows the monthly electricity consumption for the year 2022. The values were collected from the Solar Edge application that currently manages the production of the 8 installed panels. For the analyzed year, the maximum consumption occurred in December, namely, 940 kWh, and the minimum consumption in May, that is, 623 kWh. It can be seen that about 15% of the total energy consumption is covered by the energy production of the PV panels.

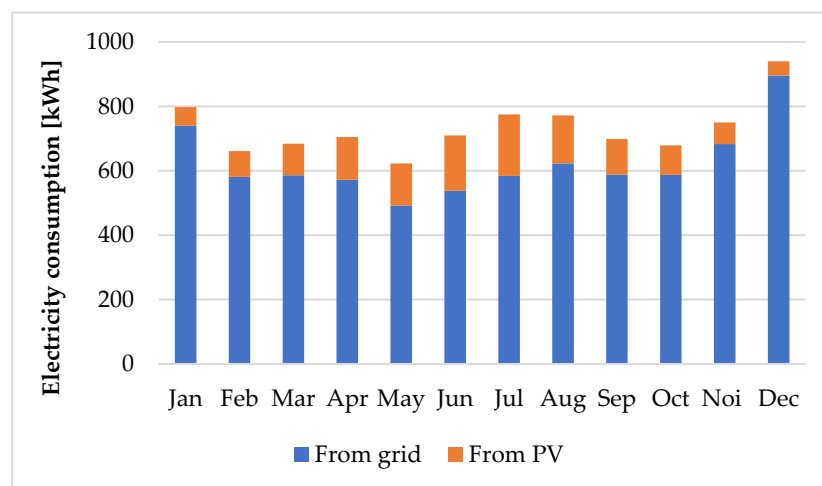


Figure 9. Monthly electricity consumption of the household.

The individualized information by category of appliances was not available at the time of the study. The authors could only operate with the global consumptions, which they processed using the real data existing in the invoices issued by the users' supplier. The electricity consumption of the household is high due to the many appliances used with long running times, such as TVs (3), computer, laptop, refrigerators (2), freezers (2), electric oven, microwave oven, electric stove, electric grill, washing machine, dryer, dishwasher, air conditioner, pool recirculation and gas plant pumps, hydrophore and other occasional consumers (such as food processor, blender, pressure cooker and vacuum cleaner). The interior and exterior lighting system also contributes to the consumption of electricity.

The chart in Figure 10 shows how the energy produced with the PV panels is used, respectively about 54% is used for their own consumption and the difference is delivered to the grid. The maximum production of electricity occurs in June, namely, 370 kWh, and in December, the electricity production is minimum, only 45 kWh.

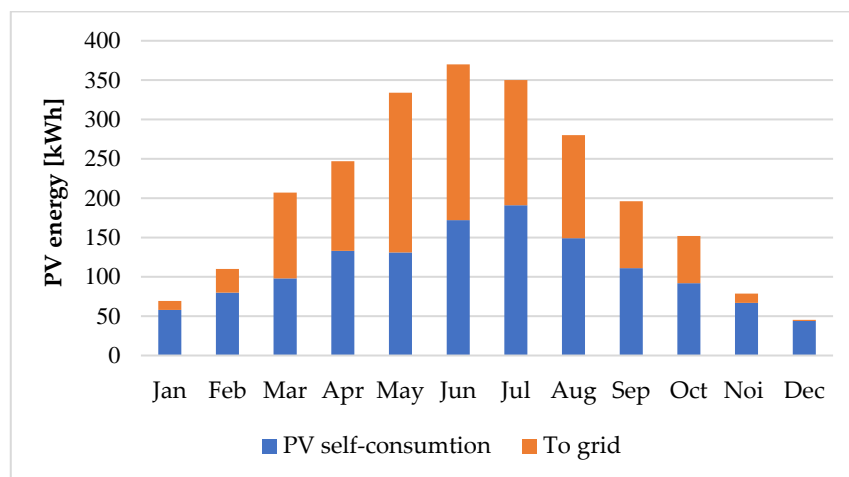


Figure 10. The use of PV energy.

3. Results

In 2021, the final energy consumption from households in Romania was the largest, accounting for approximately 35%, and both in European Union and Romania, the highest share in energy balance was for heating (64.4% in EU and 62.4% in Romania), followed by domestic hot water (14.5% in EU and 14.1% in Romania), while the third largest share was electricity for lighting and household appliances (13.6% in EU and 13.3% in Romania) [64,65]. Based on these, the first step to reduce energy consumption is to improve energy performance at the envelope level.

3.1. Building Envelope

For the current building situation, the results obtained for thermal resistance R , OHTC k - or U -value, thermal inertia index D and the coefficient of thermal massiveness m of the main building elements are summarized in Tables 4 and 5.

A series of values for minimum thermal resistance R'_{\min} and maximum thermal transmittance (maximum overall heat transfer coefficient) U'_{\max} , for buildings designed after 1 October 2010, is shown in Table 6 (after [35]). According to the specifications, these are reference values for the corrected thermal resistance (corrected thermal transmittance), which was determined taking into account the influence of thermal bridges. In the clear field assembly, the value of unidirectional thermal resistance R is much higher, and the value of unidirectional thermal transmittance is much lower. The U'_{\max} value is calculated using Formula (4).

Table 4. Summary of the results for the characteristics of the main building elements (walls).

No.	Level	Building Element Code	Building Element Type	δ (m)	R ($\text{m}^2 \cdot \text{K}/\text{W}$)	k - or U -Value ($\text{W}/\text{m}^2 \cdot \text{K}$)	D (-)	m (-)
1	Basement	PE-BAS	Reinforced-concrete exterior wall	0.326	0.379	2.640	3.229	1.064
2	Basement	PE-BA	Reinforced-concrete exterior wall	0.335	0.381	2.626	3.226	1.064
3	Ground floor	PE-BCA	AAC exterior wall	0.438	3.438	0.291	5.022	1.000
4	1st Floor	PE-CAR	Brick exterior wall	0.438	2.762	0.362	4.708	1.000
5	Ground floor/ 1st Floor	PI-CAR	Brick interior wall	0.230	0.536	1.865	2.714	1.000
6	Ground floor/ 1st Floor	PI-BA	Reinforced-concrete interior wall	0.230	0.400	2.500	2.223	1.000

Table 5. Summary of the results for the characteristics of the main building elements (floor slabs and roof).

No.	Level	Building Element Code	Building Element Type	δ (m)	R ($\text{m}^2 \cdot \text{K}/\text{W}$)	k- or U-Value ($\text{W}/\text{m}^2 \cdot \text{K}$)	D (-)	m (-)
1	Ground floor/ 1st Floor	PL-PC	Floor slab (Warm floor—parquet)	0.245	0.476	2.099	2.670	1.000
2	Ground floor/ 1st Floor	PL-PR	Floor slab (Cold floor—tiles)	0.235	0.399	2.509	2.257	1.000
3	Basement	PL-PS	Floor slab on the ground (Cold floor—tiles)	0.883	2.140	0.467	9.102	1.000
4	1st Floor	PL-E	Floor slab over the last level	0.118	1.586	0.630	1.711	1.000
5	1st Floor	PL-A	Roof	0.167	2.627	0.381	1.686	1.141

Table 6. Minimum thermal resistances R'_{\min} and maximum thermal transmittance U'_{\max} .

No.	Building Element	R'_{\min} ($\text{m}^2 \cdot \text{K}/\text{W}$)	U'_{\max} ($\text{W}/\text{m}^2 \cdot \text{K}$)
1	External walls, including walls adjacent to open joints (excluding glazed surfaces)	1.80	0.56
2	Slabs over the top level, under terraces or attics	5.00	0.20
3	Slabs over unheated basements and cellars	2.90	0.35
4	Slabs that separate the building from the outside, at the bottom (bowindos and passageways)	4.50	0.22
5	Slabs on ground (over SSL)	4.50	0.22
6	Slabs at the bottom of semi-basements or heated basements (under SGL)	4.80	0.21
7	External walls, under SGL, in semi-basements or heated basements	2.90	0.35
8	Exterior carpentry	0.77	1.30

Following the extended analysis conducted, it is noteworthy that, unfortunately, the existing structures of the building elements studied do not have the necessary characteristics to efficiently use the energy needed to heat the building in the cold season of the year (winter) or to protect the construction well enough during the warm season (summer).

For example, the outer basement wall (code PE-BA), made of reinforced concrete, in direct contact with the outside air (as well as the one below grade), does not have a thermal insulation layer, and the thermal resistance R (Table 4) is totally insufficient at present. The exterior walls on the ground floor (code PE-BCA) and 1st Floor (code PE-CAR), made of AAC and brick with vertical gaps, respectively, have a thermal resistance R estimated as having an approximately average value ($R = 3.4378 \text{ m}^2 \cdot \text{K}/\text{W}$ and $R = 2.7622 \text{ m}^2 \cdot \text{K}/\text{W}$, respectively), which can be easily increased by using another layer of thermal insulation material, which is more energy efficient and at the same time more environmentally friendly.

The same observations may be extended to other types of building elements, such as intermediate floor slabs and especially to the roof, whose thermal resistance of $R = 2.6265 \text{ m}^2 \cdot \text{K}/\text{W}$ or overall heat transfer coefficient of $k = U = 0.3807 \text{ W m}^2 \cdot \text{K}$ (Table 5 and Figure 11) are considered to be inadequate at present.

The proposals for improving the structures of the building elements had as their main objective the important reduction in heat transfer through unprotected or less-well-insulated building elements, ensuring a high degree of comfort for the building's occupants, both during the cold and warm seasons and also reducing the operating costs of the heating installation.

Thus, measures were proposed for the thermal insulation of currently unprotected building elements, for the use of ecological, environmentally friendly materials (sheep's wool), for increasing the thickness of the thermal insulation currently used (up to 25 cm), and also for insertion, where possible, in the structure of the construction elements, of

additional layers, such as a vapor barrier and anti-condensation foil, and the use of modern and esthetic materials for the execution of exterior and interior plaster.

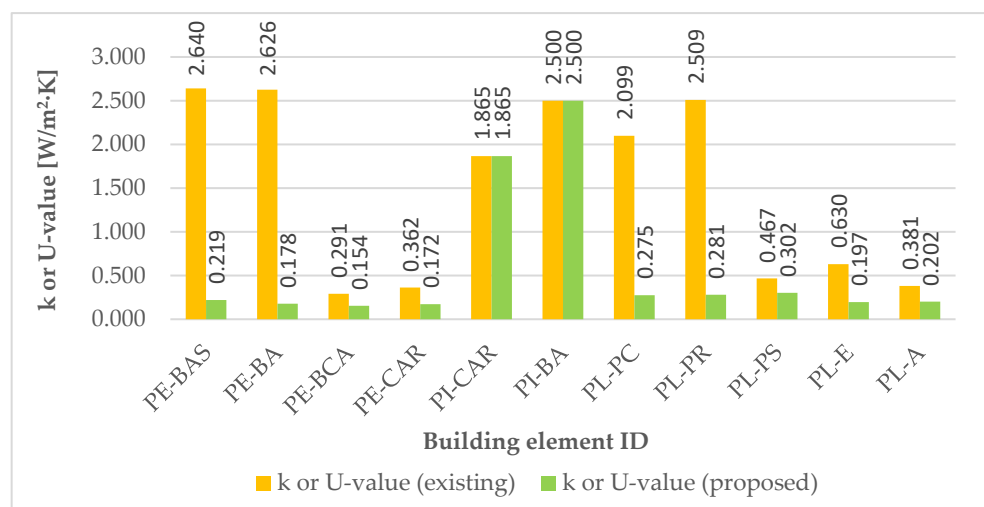


Figure 11. Overall heat transfer coefficient k- or U-value for various building elements (the existing situation and the proposed one).

The overall heat transfer coefficient k- or U-value, for the main building elements analyzed, is graphically represented in Figure 11 for the existing situation and the proposed one (improved building elements' structure).

Figure 11 shows the considerable reduction in the overall heat transfer coefficient k- or U-value for currently unprotected building elements and the decrease to about 50% in the overall heat transfer coefficient for exterior walls (PE-BCA and PE-CAR).

There is also a significant decrease in the U-value for intermediate floor slabs (PL-PC, PL-PR and PL-E) and roof (PL-A). It is important to note that all values presented in the comparative analysis are related to an area $A = 1 \text{ m}^2$ of the considered building element.

The results obtained for characteristics of glazed building elements, for the current building situation, are found in Table 7.

Table 7. Summary of the results for the characteristics of the glazed building elements.

No.	Glazed Building Element Code	Glazed Building Element Type	Position	D (-)	R ($\text{m}^2 \cdot \text{K}/\text{W}$)	k- or U-Value ($\text{W}/\text{m}^2 \cdot \text{K}$)	m (-)
1	FE	Outer window	ECE	0.500	0.330	3.030	1.200
2	UE	Exterior door	ECE	0.500	0.431	2.320	1.200
3	UI	Interior door	ECI	-	0.190	5.263	1.000

Regarding the glazed construction elements, through which significant heat losses are recorded, it was found that they at present have totally inappropriate values of thermal resistance R or overall heat transfer coefficient k- or U-value (Table 7 and Figure 12), requiring their replacement with windows and doors made with modern materials and technology.

The overall heat transfer coefficient k- or U-value for the existing and proposed situation, in the case of glazed construction elements, is graphically represented in Figure 12.

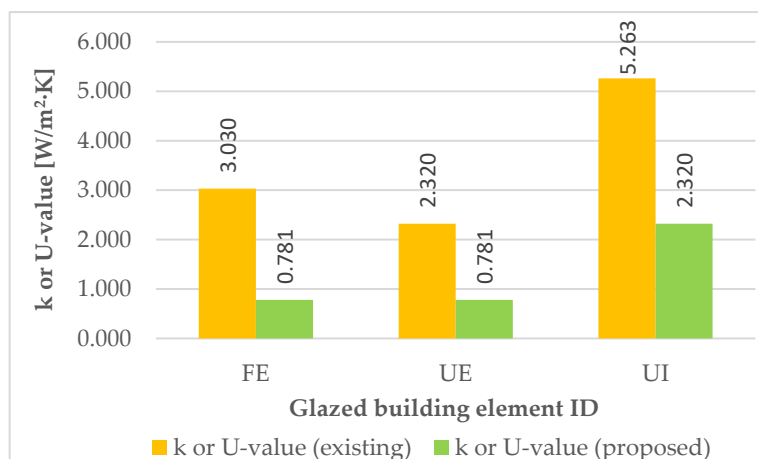


Figure 12. Overall heat transfer coefficient k or U -value for windows and doors (the existing situation and the proposed one).

3.2. Heating Load

The heating load was determined according to the methodology set out in Section 2.3, using three calculation variants for comparison. In the first calculation case (HL-01), the current structures of building elements with the characteristics presented in Tables 4, 5 and 7 were considered.

For the second case (HL-02), the characteristics of the structures of the building elements were taken into account according to their improvement proposals (Figure 11), including the replacement of glazed building elements with modern ones (Figure 12).

For both HL-01 and HL-02 cases, indoor temperatures close to those used to date by the tenants were used in the calculation for some of the rooms of the building. For example, for the office, dining room and bedroom, the indoor temperature of $\theta_i = +22\text{ }^\circ\text{C}$ was used, and for the bathroom $\theta_i = +24\text{ }^\circ\text{C}$. For the rest of the rooms, conventional indoor temperatures were used according to [34].

In the third calculation case (HL-03), the same characteristics were used as in the HL-02 case, but the indoor temperatures of all rooms of the building were considered as the conventional indoor temperatures according to [34].

The obtained results are summarized in Figure 13.

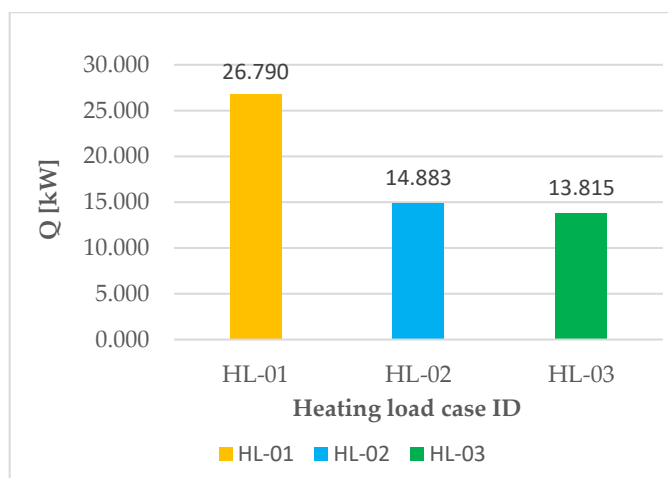


Figure 13. Comparison of the heating load cases.

The heating load for the existing situation is $Q_{HL-01} = 26.79\text{ kW}$, and in the second case, by improving the structures of the building elements, it was reduced to about

$Q_{HL-02} = 14.883$ kW. Considering the decrease in OHTC, the efficient indoor temperatures of the rooms can be reduced accordingly, and the heating load decreased even more to the value of $Q_{HL-03} = 13.815$ kW.

In what follows, case HL-03 is considered as the reference case for comparing the results obtained with those for other similar buildings. Considering that the analyzed building has an E/V (Envelope/Volume) ratio of $E/V = 0.717$, the overall coefficient G of the thermal insulation of the building has a much lower value than the maximum normed G_N according to [35] ($G = 0.407$ W/m³·K < $G_N = 0.743$ W/m³·K). The annual heating load is 15.05 kWh/m³·year or an equivalent value of about 47.04 kWh/m²·year, which also is a much lower value than the annual standard heating load normed $Q_{N2} = 27.94$ kWh/m³·year or $Q_{N2} = 87.3$ kWh/m²·year, determined according to [35].

For the DHW preparation, a number $n_p = 4$ persons was taken into account, with a usual DHW demand per person and day of $C_{zn} = 50$ L/pers·day, a DHW temperature of $t_{DHW} = 45$ °C, an average temperature of the supply (cold water) of $t_{ar} = 10$ °C and a regular preparation time of $\tau = 8$ h, resulting in a heating demand of $Q_{DHW} = 1.01$ kW, equivalent to an energy consumption of 8.083 kWh or about 11.3 kWh/m²·year. The variation of the heating demand for the DHW preparation with respect to time is shown in Figure 14.

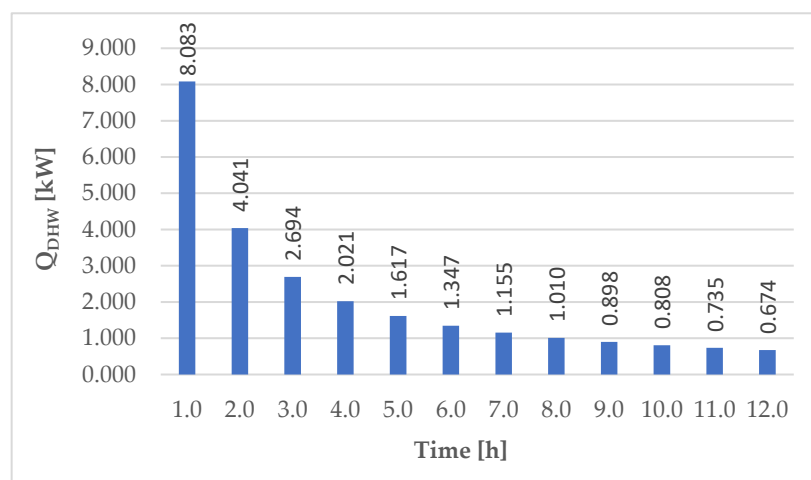


Figure 14. Heating demand with respect to time for the DHW preparation.

It can be seen from Figure 14 that, if the energy source, using its own automation, uses a higher thermal output, the DHW preparation time can be greatly reduced. For example, for a thermal load of 8 kW, the DHW preparation time is reduced to about 1 h (for higher powers even less), thus increasing the comfort of the building occupants in terms of DHW use. Considering a safety factor $f = 2$, the result is the required volume $V = 280$ L for the DHW cylinder.

In the current situation, the heating and hot water preparation are conducted using a 38 kW condensing gas boiler and a 150 L hot water tank. The distribution pipes for heating are made of copper and the heating elements are aluminum radiators, sized for flow/return temperatures of 70/50 °C. The distribution pipes on the domestic hot water are made of polypropylene random copolymer (PPR), insulated only in the basement with a 9 mm thickness. It is proposed to rehabilitate the house and replace the gas boiler with a heat pump for heating and hot water preparation, with a buffer tank for heating and hot water tank for domestic hot water. Instead of the heating elements, an underfloor heating system is designed for flow/return temperatures of 35/30 °C with 16×2 mm Pe-X/Al/Pe-X pipes in a bifilar layout with a peripheral area (using smaller laying intervals in the peripheral areas along the external walls). Additionally, heat distribution conduits and heating-system risers and conduits installed in the basement will be replaced with PPR pipes (16×2.2 mm, 20×2.8 mm and 25×3.5 mm dimensions, insulated with a 10 mm or 20 mm thickness and a thermal conductivity of $\lambda = 0.035$ W/m·K, based on where the heating conduits are laid).

3.3. Heat Pump System Simulations

Considering the important role that natural gas plays in terms of heating and hot water preparation in Romania (34.5% for heating and 59% for domestic hot water in 2021) to accelerate the green transition [64,66], the consumers from our country will have to invest in technologies related on renewable sources of energy, such as heat pumps.

Based on the simulations conducted with the GeoT*SOL software, the following were determined for the two heat pump systems: energy taken from the source (air or ground), energy generated for heating and DHW preparation, electricity consumption and SPF.

In the case of ASHP, the energy taken from the source (10,094 kWh/year) depends on the variation of the outside air ($-18 \dots +35 \text{ }^{\circ}\text{C}$), as can be seen in the Figure 15, and represents 65% of the energy supplied by the HP system.

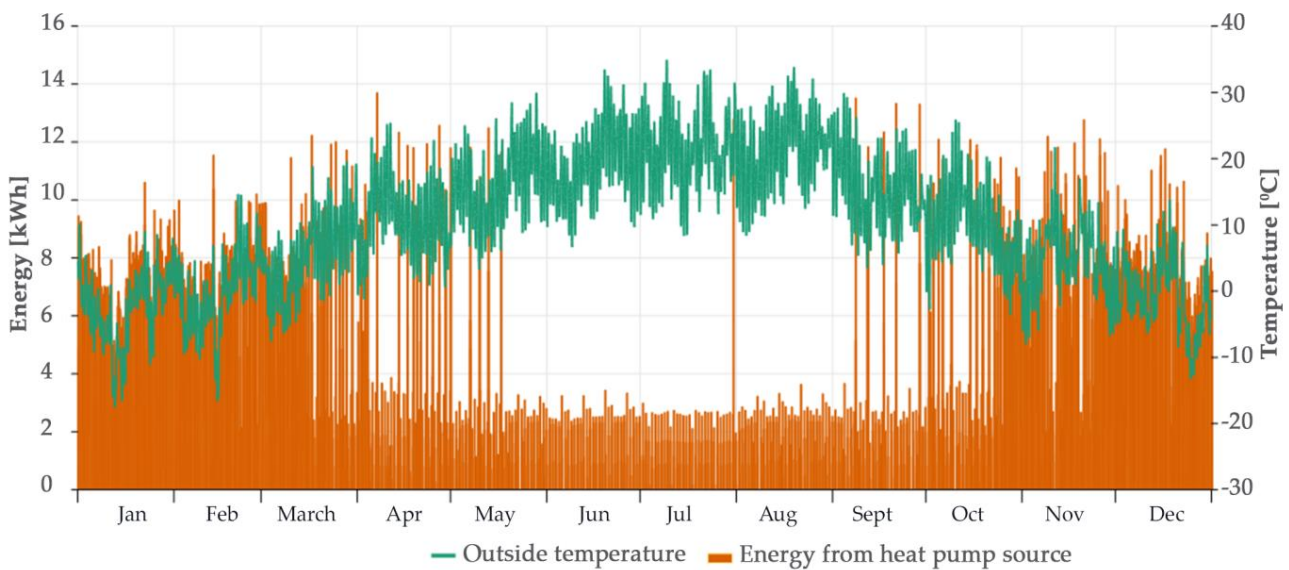


Figure 15. Hourly outside temperature and thermal energy from the outside (ASHP).

In the case of GSHP, since the temperature of the heat pump brine inlet shows much smaller variations between -5 and $+7 \text{ }^{\circ}\text{C}$, the performance of the system is better, and the amount of energy taken from the ground reaches an annual value of 11,637 kWh (as can be seen in Figure 16), representing 75% of the energy supplied by the HP system.

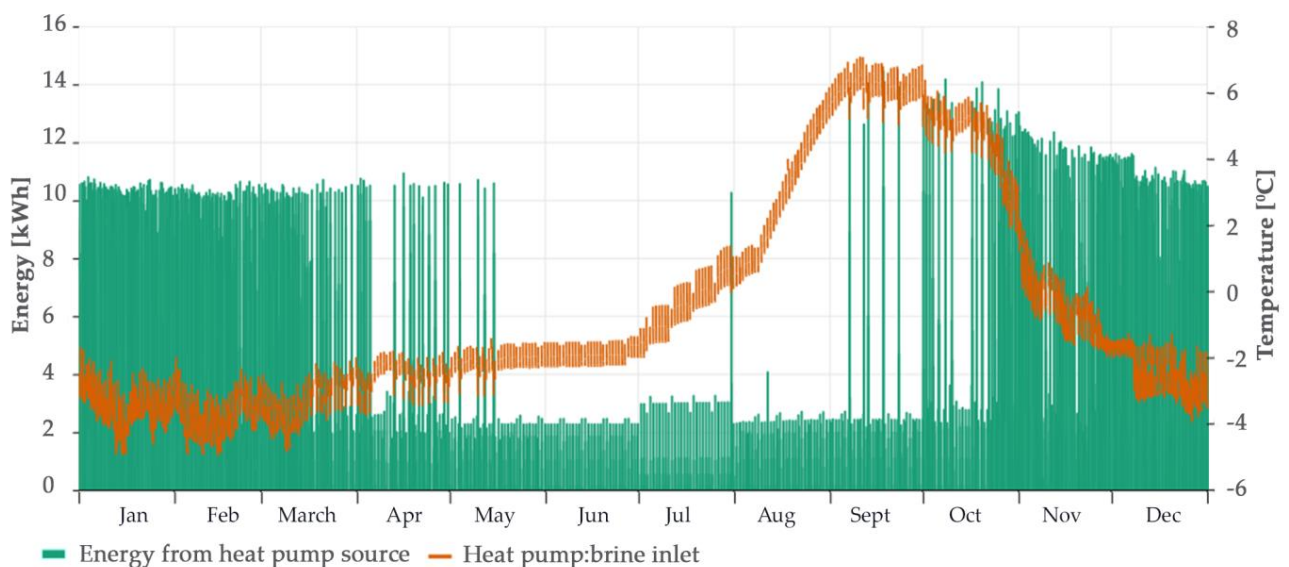


Figure 16. Hourly brine inlet temperature and thermal energy from the ground (GSHP).

For both systems, 81% of the energy generated is used for heating and 19% for DHW preparation.

The annual electricity consumptions resulting from the two analyzed cases and the seasonal performance factor are presented in Figure 17. As it can be seen, the highest electrical consumption was for ASHP (5452 kWh/year), while for the GSHP with geothermal collectors, the consumption was 23% lower. In terms of SPF, the annual value reported for the entire heat pump system (considering all the electrical consumptions for the compressor, heating element and auxiliary energy) was 3.73 for GSHP and 2.85 for ASHP, about 24–26% lower than the SPF for the HP.

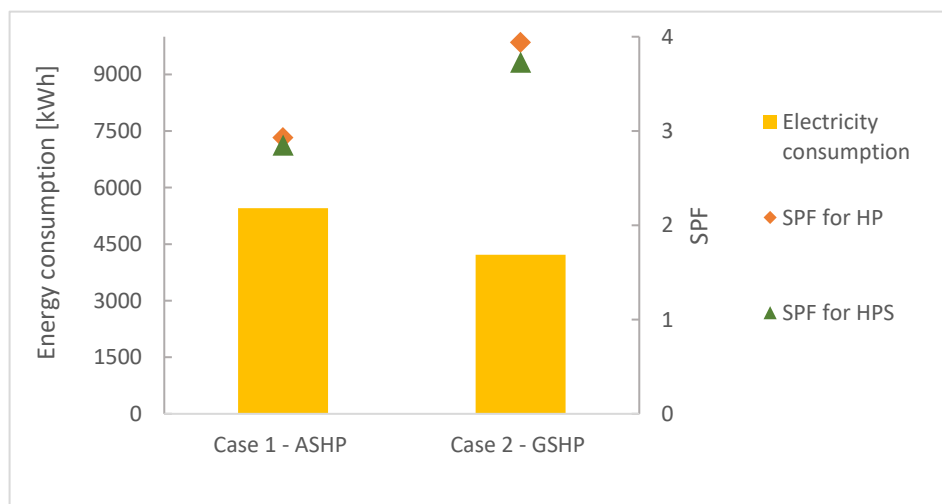


Figure 17. Annual electricity consumption and annual average seasonal performance factors for ASHP and GSHP.

Analyzing the distribution of annual electrical consumption, it was observed that, for the ASHP, the power consumption of the heat pump compressor represents 96% and the remaining 4% is recorded for the heating element, while for the GSHP, 94% was for the heat pump compressor and 6% for the auxiliary energy (Figure 18).



Figure 18. Electrical energy distribution for (a) ASHP and (b) GSHP.

Collecting the simulated monthly values from the software (Figure 19), it was noticed that, in the case of using an ASHP, to cover the energy requirement in January and February,

the heating element is operated, thus increasing the electricity consumption to 1355 kWh in January and 837 kWh in February and so decreasing the SPF of the heat pump system. In the case of GSHP, the auxiliary energy (external pump on the side of the heat source of the HP) is added to the heat pump consumption (the compressor) every month, with the largest values being recorded in January–March and November–December.

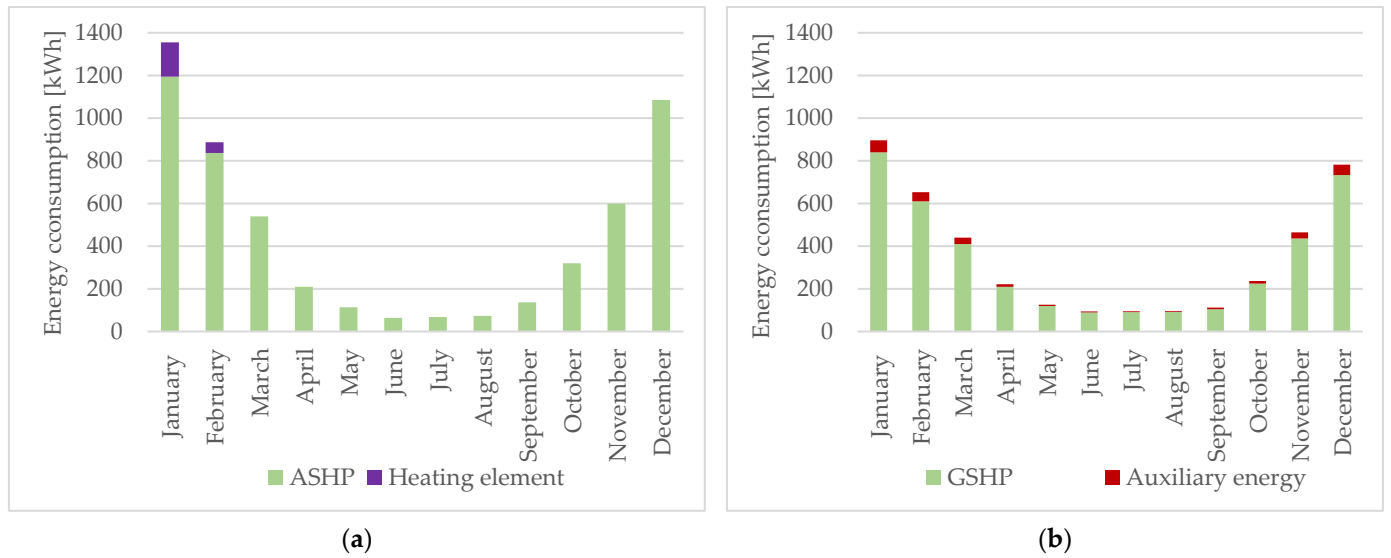


Figure 19. Electrical energy for: (a) ASHP (case 1); (b) GSHP (case 2).

Analyzing the hourly variation of the electrical energy consumption compared to the variation of the SPF (Figures 20 and 21), it was noticed that: in the case of ASHP in the period with the highest electrical consumption of the heat pump and the heating element (January–February), the SPF of the HP system decreased to values between 1 and 1.5, while in the spring and autumn seasons, the SPF exceeded the value of 4, with the largest value recorded being 4.35 in August; in the case of the GSHP, the SPF of the HP system varied between 2.5 (in the winter season) and even values over 6.

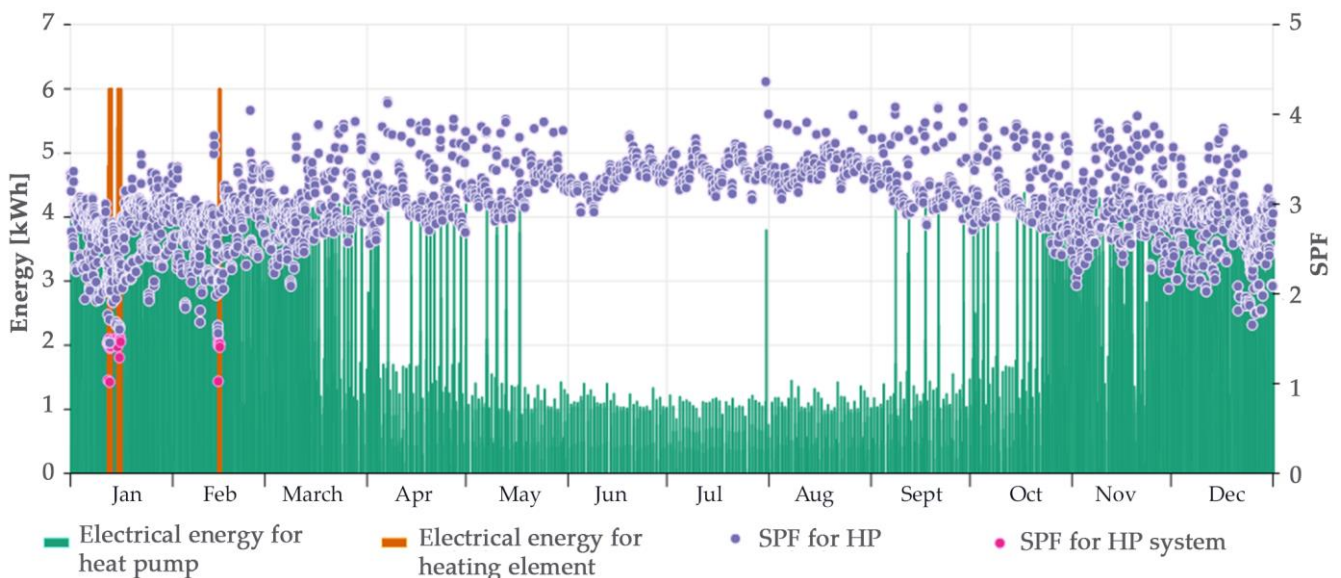


Figure 20. Hourly electrical energy consumption and SPF (ASHP).

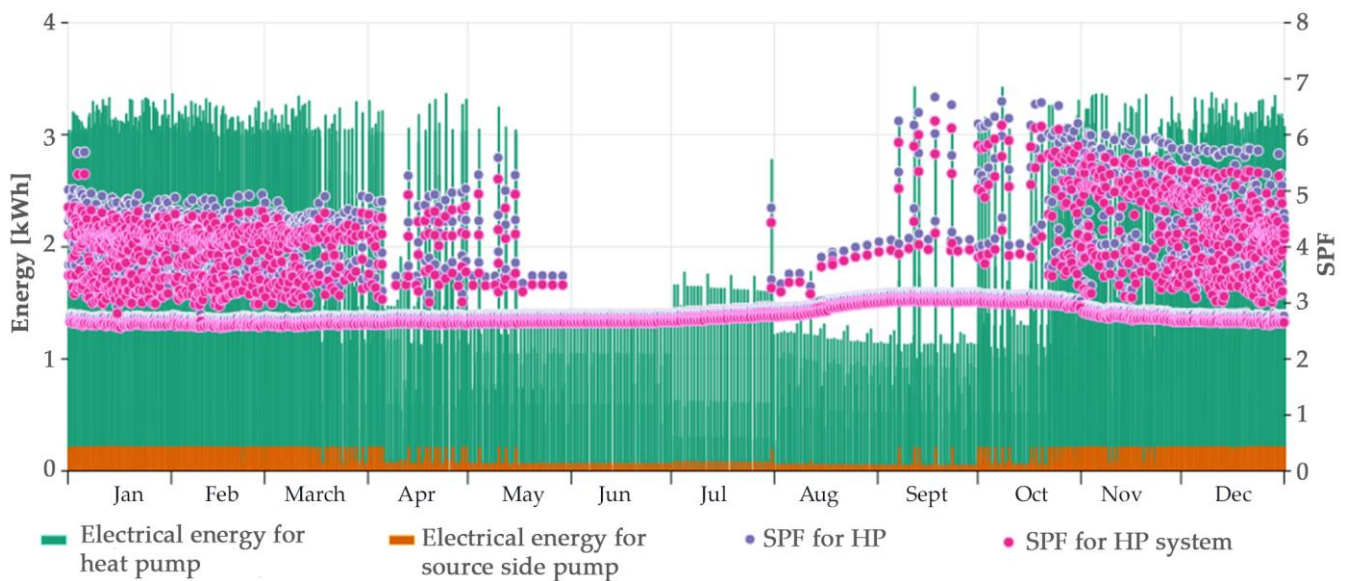


Figure 21. Hourly electrical energy consumption and SPF (GSHP).

When using a GSHP, all the energy required for space heating and DHW is covered by the heat pump (auxiliary energy representing the power consumption for the source side pumps), with the power consumption being around 20% smaller in the period of January–March and September–December than in the case of using an ASHP.

Based on the gas consumption recorded in 2022 for the existing heating plant (case 0) and the electricity consumption simulated with the GeoT*SOL software for the proposed system, in Figure 22 (ASHP (case 1) and GSHP (case 2)), the percentage reductions in energy consumption are presented monthly. As seen in the figure, by replacing the gas-based system with an air- or ground-source heat pump, the annual energy consumption is reduced by 88% for ASHP and 91% for GSHP, with the largest decreases being expected in the case of implementing a GSHP (between 85–93% in the period of January–May and September–December). All these energy reductions, compared to the present conventional natural gas heating system, will lead to a reduction in energy operating costs and thus monthly energy bills for heating.

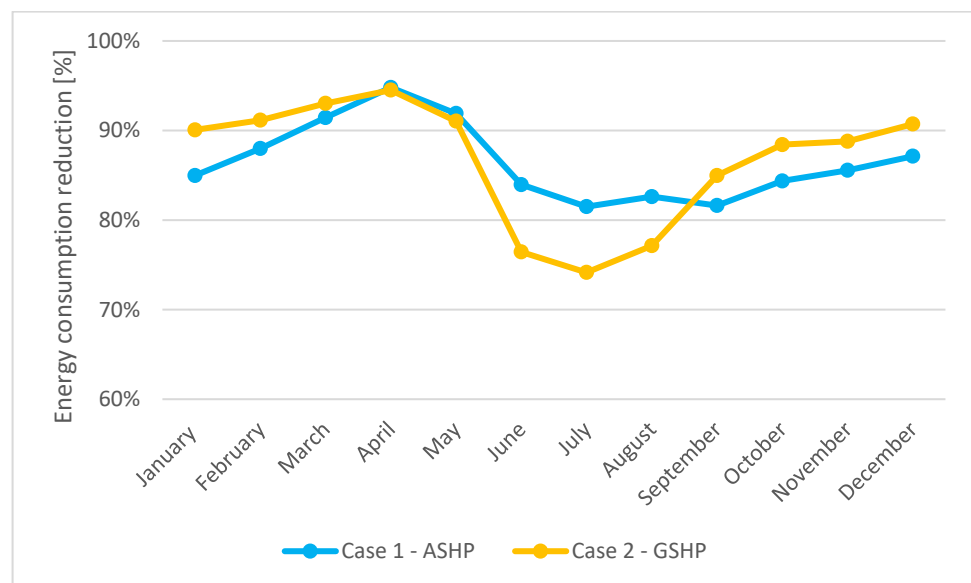


Figure 22. Electrical energy reductions for the ASHP and GSHP systems compared with the existing system.

3.4. PV Panels

The subsidies offered by the Romanian state through the Green House program and the extra funding options through the REPowerEU plan promote the installation of photovoltaic systems and help prosumers to recover their investment faster [67].

In this context, in order to increase the percentage of electricity produced from solar energy, we proposed the addition of 24 PV panels of the same type, having the technical characteristics specified in Table 8.

Table 8. Technical characteristics of the PV panels.

No.	Parameter	Value
1	Maximum power	395 W
2	Open-circuit voltage	49.45 V
3	Short-circuit current	10.35 A
4	Voltage at point of maximum power	41.07 V
6	Current at point of maximum power	9.62 A
7	Module efficiency	19.6%
8	Weight	23.5 kg
9	Length	2008 mm
10	Width	1002 mm
11	Temperature range	−40 to 85 °C

The PV*SOL Premium program can calculate the shading areas that were taken into account when placing the 32 panels, including the existing 8, respectively 16 on each side (Figure 23).

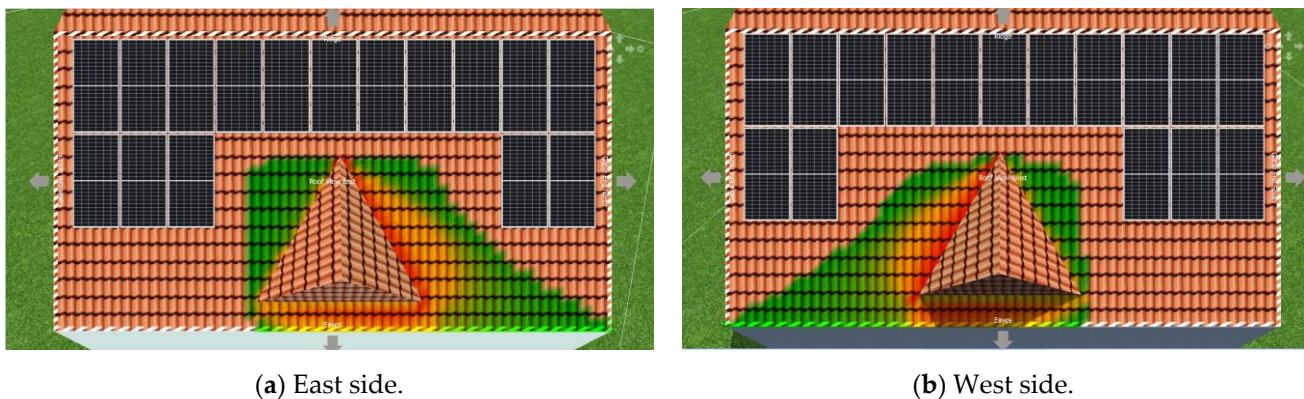


Figure 23. Location of the proposed PV system.

The chart in Figure 24 shows the results of the simulations performed with PV*SOL Premium regarding the electricity production of the proposed PV system with an installed power of 12.64 kW compared to the existing PV system with an installed power of 3.16 kW. It is observed that the energy production using the proposed system is 5.23 times higher than that with the existing system, reaching a maximum production of 1672 kWh in June.

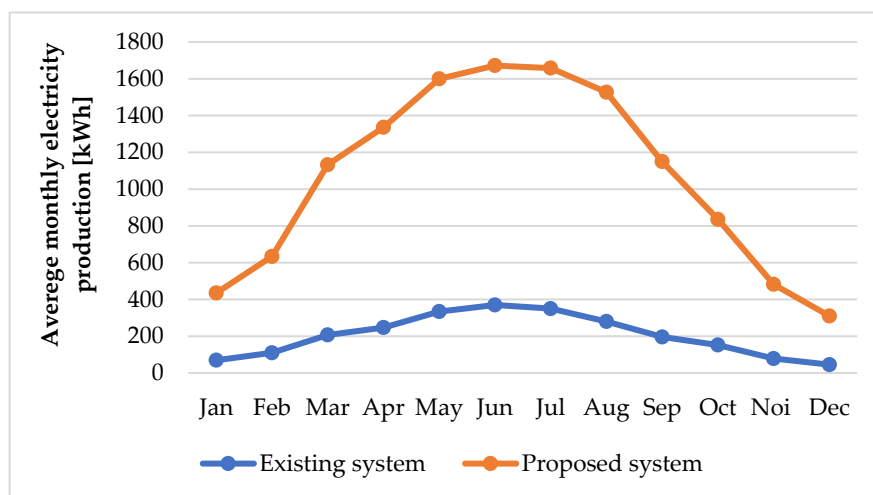


Figure 24. Average monthly electricity production.

In the chart in Figure 25, a comparison was conducted between the simulation results regarding the electricity production obtained with the PV panels and the electricity consumption, including the consumption generated by the heat pump in the two proposed cases: case 1 with an air-source heat pump and case 2 with a ground-source heat pump with geothermal collectors. As it can be seen in Figure 25, the electricity requirement of the house is not fully covered, the deficit being greater in the cold season months. One mentions the fact that, by installing the heat pump, the consumption of electricity increases, instead, heating using fossil fuel plant is no longer used.

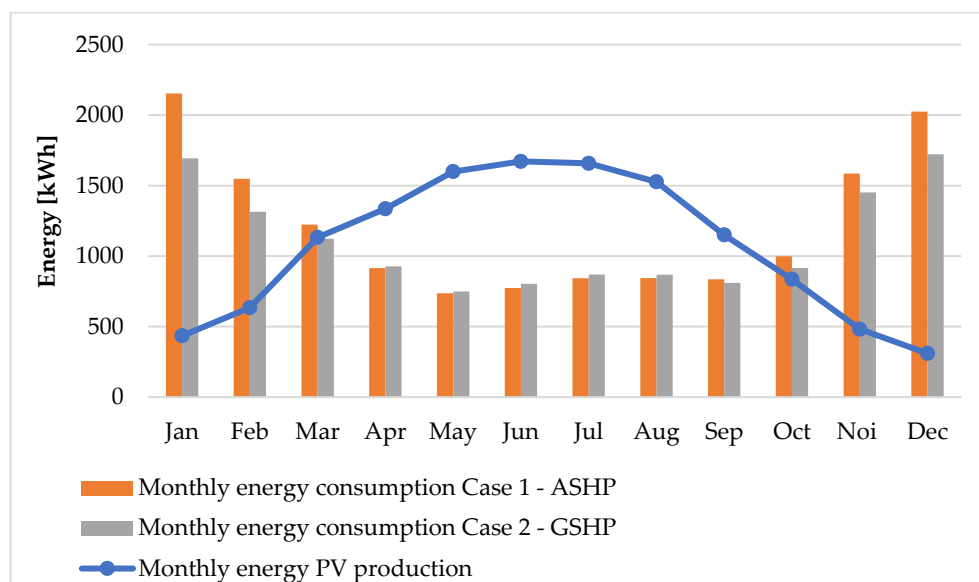


Figure 25. Energy production vs. energy consumption.

Figure 26 shows how the energy consumption is covered in the two proposed cases. In case 1 with ASHP (Figure 26a), the energy consumption is covered by the production of PV panels to an extent of 34.3%, the difference of 65.7% being supplied by the grid.

In case 2 with GSHP (Figure 26b), the energy produced by the PV panels covers 36.3% of the energy consumption, the grid providing the other 63.7%.

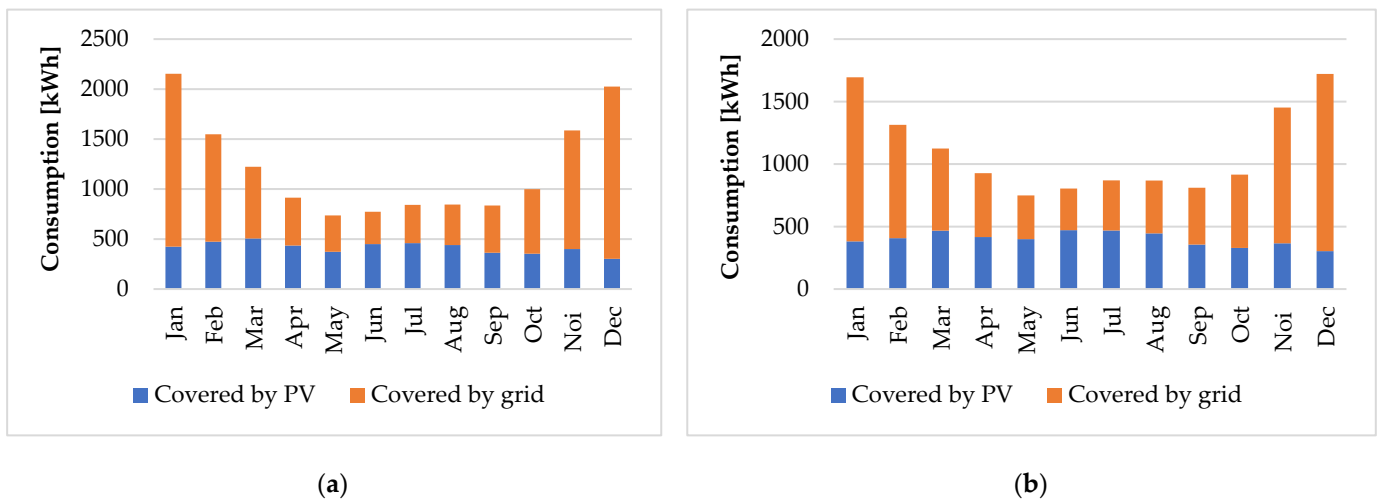


Figure 26. The coverage of consumption: (a) case 1 with ASHP; (b) case 2 with GSHP.

The charts in Figure 27 show how the energy produced by the PV system is used in the two proposed cases. Thus, it can be seen that most of the energy produced is sent into the grid, 61% in case 1 and 62% in case 2. This is due to the fact that the high energy production from PV, which occurs in the spring and summer months, is not in agreement with the high energy demand that occurs in the cold months of the year.

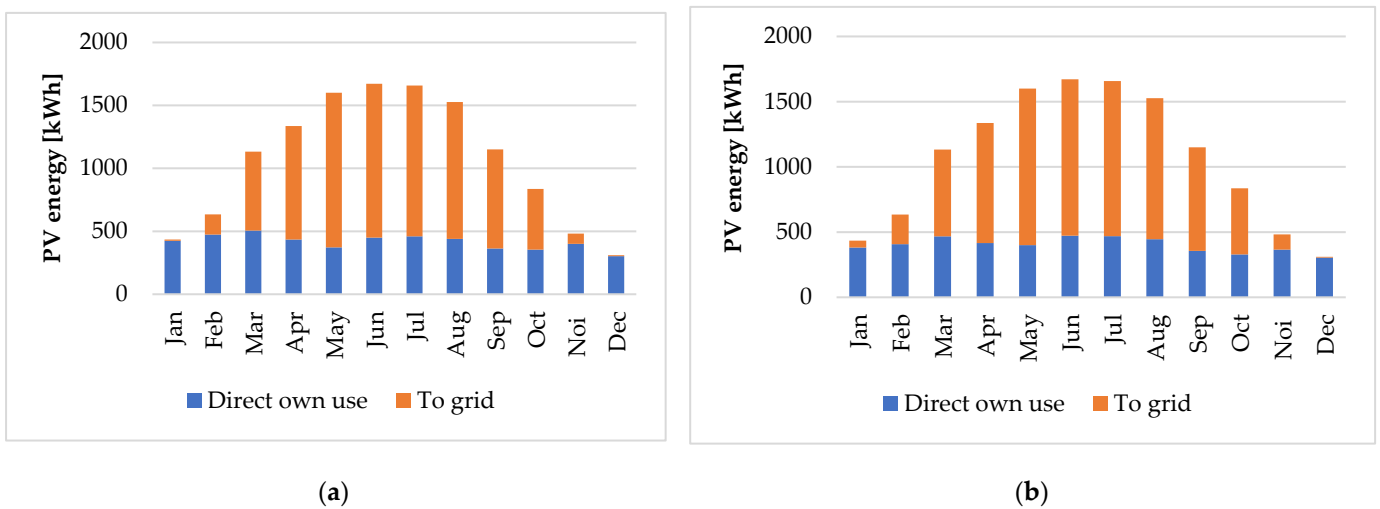


Figure 27. The use of PV energy: (a) case 1 with ASHP; (b) case 2 with GSHP.

4. Discussion

While in Romania fossil fuels are the dominant energy source and under a quarter of primary energy comes from low-carbon sources, its electricity mix for 2022 was quite balanced: around 25.3% hydropower, 20% nuclear, 18.5% coal, 17.6% gas, 12.6% wind, 3.2% solar, 1.6% oil and 1.2% bioenergy, with the share of renewable sources of energy in electricity mix exceeding 42% [1].

Between the second half of 2021 and the same period for 2022, both electricity and gas prices grew enormously, with our country recording the highest increase in the price of electricity among all EU members (112%) and the second largest rise for gas price (165%) [68].

Taking these things into account, thermal rehabilitation to reduce energy consumption together with the transition from gas heating to a heat pump powered by a solar PV system will improve energy efficiency, increase the share of solar energy, reduce fossil fuel consumption and reduce carbon emissions but also costs, being in line with the energy

and climate objectives and the REPowerEU plan [66]. Additionally, according to the review conducted by Mohammed et al. [69] for residential buildings, the most effective mechanisms to improve energy efficiency and to model sustainable cities are solar energy and building's envelope thermal performance.

Analyzing Figure 12, one immediately notices the positive effect of the proposed changes for the structures of the building elements, by using efficient thermal insulation materials that are friendly to the environment and the use of modern glazed building elements with a high thermal resistance or an equivalent low OHTC.

The heating load for case HL-02 represents only about 55.55% of the heat requirement for the HL-01 case and, moreover, reducing the indoor temperatures to the conventional values according to [34] for HL-03 case leads to an even lower value of the heating load Q_{HL-03} , representing only about 51.56% of that corresponding to the HL-01 case. The annual heating load expressed in kWh/m³·year or the equivalent for typical comparisons in kWh/m²·year represents only about 53.88% of the annual standard heating load normed by [35].

To meet the thermal energy needed by the household from this case study, the proposed heat pump system can provide many advantages compared to the current classic heating system based on natural gas: the elimination of fossil fuel dependence (in this case, from natural gas), significant energy and costs savings by reducing consumption and of course reducing primary energy, and the negative impact on the environment by minimizing CO₂ emissions.

According to the SolarPower Europe report [20], an average European home equipped with heat pumps powered by PV systems brought savings between 62% and 84% on energy bills in 2022, compared with a house using a natural gas boiler for heating and obtaining electricity from the grid. From the study conducted by Bellos et al. [70] for a building in Athens resulted that, for the current electricity price (0.2 EUR/kWh), the system with an air-source heat pump and PV panels had the minimum investment costs. Comparing the heat pump systems proposed in our study to replace the existing heating system and considering the current national price for natural gas (0.063 EUR/kWh) and electricity (0.26 EUR/kWh), the most significant reductions are occurring in the energy operating costs for heating: 49% in the case of the air-source heat pump and 60% for the ground-source heat pump, percentages that will be improved by combining these heat pumps with photovoltaic systems.

According to Zhang et al. [71], both solar-assisted air-source and ground-source heat pumps could considerably reduce primary energy consumption, but to achieve a high performance, it is recommended to use low-temperature heating instead of radiators, air-source heat pump for hot climates and ground-source heat pumps for cold climates.

Based on the simulations performed with GeoT*SOL, the primary energy savings and avoided CO₂ emissions determined for the two heat pump systems, compared to a classic heating system, revealed primary energy reductions of over 9920 kWh for ASHP and 13,590 kWh for GSHP and CO₂ emissions reductions of over 2450 kgCO₂eq for ASHP and 3360 kgCO₂eq for GSHP.

Although the total annual electricity produced by the PV system represents 88% of the annual consumption in case 1 and 96% of the annual consumption in case 2, in fact, only 39% of the energy produced by the PV system is used for own consumption in case 1 and 37.7% in case 2, as shown in Figure 21.

A first limitation of this paper consists in the fact that the use of these systems is not stable, being influenced and affected by the climatic and geographical conditions specific to the site area: solar radiation, air temperature and soil characteristics. Another limitation is the access to different simulation software, and the differences and compatibility between them.

Likewise, in the case of installing PV panels, there are limitations regarding the space available on the roof and the weight supported by the existing structures. In addition, when equipping with PV panels, one must also consider the shaded areas that can decrease

the efficiency of the panels. In this case, the PV*SOL Premium program helps the user in choosing the most favorable solution.

At present, there are much better performing panels with a power of about 600 W, but since the house was under monitoring after it was equipped with eight panels in 2021 through the Green House program, and in order not to disturb the operation of the system, we chose panels of the same type, so that they can be integrated on each side and an inverter can be connected. In the near future, we aim to make comparative simulations on the several ways of connecting photovoltaic panels and inverters to analyze the possibility of storing energy in periods without consumption and also equipping with optimizers to reduce consumption from the national electricity grid in cold periods, when the heat pump registers the highest electrical consumption.

5. Conclusions

Combining the results of the heating requirements for heating (47.04 kWh/m²·year) and DHW preparation (11.3 kWh/m²·year), an index of the required energy per m² of useful area of about $Q_{1m^2} = 58.34$ kWh/m²·year or an annual consumption of 15,233 kWh/year was obtained, which places the proposed modernized building in the low-energy building consumption category.

Taking into account all the improvements regarding energy efficiency, the use of solar energy, CO₂ emissions reduction and also operating costs, the fact that the investment cost for an ASHP is lower than that for a GSHP (to the purchase price adding the cost of excavation) and benefits from easier installation, the system with an ASHP powered by PV systems is a suitable choice for the occupants of the household studied.

Comparing the results obtained from simulations in PV*SOL Premium with the data related to the electricity and gas consumption from the existing situation, considering the gas and electricity prices mentioned above, it resulted that the implementation of the two proposed solutions considerably lowered the cost of household maintenance. Thus, by the addition of 24 panels and installing a heat pump, the annual bill decreased by 47% in case 1 with ASHP and by 53% in case 2 with GSHP in relation to the existing situation, namely, with eight PV panels and a gas plant for heating and domestic hot water. However, given that there is a bidirectional meter, if at the end of the year a balance is established between the energy consumed from the grid and the energy delivered to the grid, the annual savings increase significantly, i.e., 89% in case 1 and 97% in case 2, compared to the current case.

All the results of this study were received with great interest by the owners of the household, being appreciated as valuable in order to reduce energy consumption and operating costs of installations, thus concluding, globally, to improve the overall energy efficiency of the building.

At present, the final decision of the owners is awaited regarding the investment necessary to make the planned changes to the structures of the building elements, the addition of supplementary PV panels and the equipping with modern air–water heat pumps for heating and DHW preparation.

Author Contributions: Conceptualization, C.M., G.C. (Georgiana Corsiuc), R.M. and G.C. (Gelu Chisăliță); methodology, C.M., G.C. (Georgiana Corsiuc), R.M. and G.C. (Gelu Chisăliță); software, G.C. (Georgiana Corsiuc), R.M. and G.C. (Gelu Chisăliță); validation, C.M., G.C. (Georgiana Corsiuc), R.M. and G.C. (Gelu Chisăliță); formal analysis, C.M., G.C. (Georgiana Corsiuc), R.M. and G.C. (Gelu Chisăliță); investigation, C.M., G.C. (Georgiana Corsiuc), R.M. and G.C. (Gelu Chisăliță); resources, C.M., G.C. (Georgiana Corsiuc), R.M. and G.C. (Gelu Chisăliță); data curation, G.C. (Georgiana Corsiuc) and R.M.; writing—original draft preparation, C.M., G.C. (Georgiana Corsiuc), R.M. and G.C. (Gelu Chisăliță); writing—review and editing, C.M., G.C. (Georgiana Corsiuc), R.M. and G.C. (Gelu Chisăliță); visualization, C.M., G.C. (Georgiana Corsiuc), R.M. and G.C. (Gelu Chisăliță); supervision, C.M.; project administration, C.M.; funding acquisition, not applicable. All authors have read and agreed to the published version of the manuscript.

Funding: This research received no external funding.

Data Availability Statement: Not applicable.

Conflicts of Interest: The authors declare no conflict of interest.

References

1. Energy—Our World in Data. Available online: <https://ourworldindata.org/energy> (accessed on 20 June 2023).
2. *Synthesis Report Of The IPCC Sixth Assessment Report (Ar6)*; The Intergovernmental Panel on Climate Change (IPCC): Interlaken, Switzerland, 2003.
3. Gielen, D.; Boshell, F.; Saygin, D.; Bazilian, M.D.; Wagner, N.; Gorini, R. The Role of Renewable Energy in the Global Energy Transformation. *Energy Strategy Rev.* **2019**, *24*, 38–50. [[CrossRef](#)]
4. Kannan, N.; Vakeesan, D. Solar Energy for Future World: A Review. *Renew. Sustain. Energy Rev.* **2016**, *62*, 1092–1105. [[CrossRef](#)]
5. Silvi, C. Solar Energy. In *2004 Survey of Energy Resources*; Elsevier Science: Amsterdam, The Netherlands, 2004; pp. 295–334.
6. About Solar Energy | SEIA. Available online: <https://www.seia.org/initiatives/about-solar-energy> (accessed on 20 June 2023).
7. Mârza, C.; Hoțupan, A.; Moldovan, R.; Corsiuc, G. *Surse Neconvenționale de Energie (Unconventional Energy Sources)*; U.T. PRESS: Cluj-Napoca, Romania, 2013.
8. Mârza, C.; Corsiuc, G.; Pop, A. Case Study Regarding the Efficiency of Electricity Generation Using Photovoltaic Panels. In *Proceedings of the International Multidisciplinary Scientific GeoConference, SGME, Sofia, Bulgaria, 20 June 2018*.
9. Năstase, G.; Șerban, A.; Dragomir, G.; Ionuț Brezeanu, A.; Bucur, I. Photovoltaic Development in Romania. Reviewing What Has Been Done. *Renew. Sustain. Energy Rev.* **2018**, *94*, 523–535. [[CrossRef](#)]
10. Amjahdi, M.; Lemale, J. *Energia Solară Termică Și Fotovoltaică (Thermal and Photovoltaic Solar Energy)*; Matrix Rom: București, Romania, 2012.
11. Bălan, M. *Energii Regenerabile (Renewable Energies)*; UT Press: Cluj-Napoca, Romania, 2007.
12. Duffie, J.; Beckman, W. *Solar Engineering of Thermal Processes*, 4th ed.; John Wiley & Sons: Hoboken, NJ, USA, 2013.
13. Li, H.; Lian, Y.; Wang, X.; Ma, W.; Zhao, L. Solar Constant Values for Estimating Solar Radiation. *Energy* **2011**, *36*, 1785–1789. [[CrossRef](#)]
14. Popescu, M.O.; Popescu, C.L. *Surse Regenerabile de Energie Vol.1: Principii Și Aplicații (Renewable Energy Sources. Vol.1. Principles and Application)*; Electra: București, Romania, 2010; Volume 1.
15. International Energy Agency. *Photovoltaic Power Systems Programme Snapshot of Global PV Markets 2023 Task 1 Strategic PV Analysis and Outreach PVPS*; International Energy Agency: Paris, France, 2022.
16. Pater, S. Increasing Energy Self-Consumption in Residential Photovoltaic Systems with Heat Pumps in Poland. *Energy* **2023**, *16*, 4003. [[CrossRef](#)]
17. Rosenow, J.; Gibb, D.; Nowak, T.; Lowes, R. Heating up the Global Heat Pump Market. *Nat Energy* **2022**, *7*, 901–904. [[CrossRef](#)]
18. International Energy Agency. *World Energy Outlook Special Report The Future of Heat Pumps*; International Energy Agency: Paris, France, 2012.
19. European Climate Foundation; European Alliance to Save Energy (EU-ASE). *Buildings Europe's Net-Zero Future. Why the Transition to Energy Efficient and Electrified Buildings Strengthens Europe's Economy*; European Climate Foundation: Brussels, Belgium, 2022.
20. SolarPower Europe. *Solar Powers Heat 2023. How Solar PV Empowers Households to Turn down Fossil Gas and Save on Energy Bills*; SolarPower Europe: Brussels, Belgium, 2023.
21. Hou, G.; Taherian, H. Performance Analysis of a Hybrid Ground Source Heat Pump System Integrated with Liquid Dry Cooler. *Appl. Therm. Eng.* **2019**, *159*, 113830. [[CrossRef](#)]
22. Hou, G.; Taherian, H.; Li, L.; Fuse, J.; Moradi, L. System Performance Analysis of a Hybrid Ground Source Heat Pump with Optimal Control Strategies Based on Numerical Simulations. *Geothermics* **2020**, *86*, 101849. [[CrossRef](#)]
23. Hou, G.; Taherian, H.; Li, L. A Predictive TRNSYS Model for Long-Term Operation of a Hybrid Ground Source Heat Pump System with Innovative Horizontal Buried Pipe Type. *Renew. Energy* **2020**, *151*, 1046–1054. [[CrossRef](#)]
24. *Communication from the Commission to the European Parliament, the Council, the European Economic and Social Committee and the Committee of the Regions—EU Solar Energy Strategy COM(2022) 221 Final*; European Commission: Brussels, Belgium, 2022.
25. Opinion of the European Economic and Social Committee on Communication from the Commission to the European Parliament, the Council, the European Economic and Social Committee and the Committee of the Regions—EU Solar Energy Strategy (COM(2022) 221 Final) and Commission Recommendation on Speeding up Permit-Granting Procedures for Renewable Energy Projects and Facilitating Power Purchase Agreements (C(2022) 3219 Final). Available online: <https://eur-lex.europa.eu/legal-content/EN/TXT/?uri=CELEX:52022AE3515> (accessed on 21 June 2023).
26. *The 2021–2030 Integrated National Energy and Climate Plan*; European Commission: Brussels, Belgium, 2020.
27. Romania—Energy. Available online: <https://www.trade.gov/country-commercial-guides/romania-energy> (accessed on 20 June 2023).
28. Romania Solar Photovoltaic (PV) Power Market Outlook 2023÷2032 with Trends, Investments, Financial Model, Analysis, Forecast—Renewable Market Watch. Available online: <https://renewablemarketwatch.com/news-analysis/488-romania-solar-photovoltaic-pv-power-market-outlook-2023-2032-with-trends-investments-financial-model-analysis-forecast> (accessed on 20 June 2023).

29. JRC Photovoltaic Geographical Information System (PVGIS)—European Commission. Available online: https://re.jrc.ec.europa.eu/pvg_tools/en/#TMY (accessed on 29 June 2023).
30. PV*SOL Premium | Photovoltaic Design and Simulation. Available online: <https://valentin-software.com/en/products/pvsol-premium/> (accessed on 29 June 2023).
31. I.P.C.T.C.C. C 107/3-1997; Normativ Privind Calculul Termotehnic al Elementelor de Construcție Ale Clădirilor (Normative Regarding the Thermotechnical Calculation of Building Construction Elements). Institutul de Proiectare, Cercetare și Tehnică de Calcul în Construcții (Institut of Design, Research and calculation Technique in Constructions): București, Romania, 1997.
32. A.I.I.R. *Enciclopedia Tehnică de Instalații. Manualul de Instalații. Instalații de Încălzire (Technical Encyclopedia of Installations. Manual of Installations. Heating Installations)*, 2nd ed.; Artecno: București, Romania, 2010.
33. I.R.S. SR 1907-1:1997; Instalatii de Incalzire. Necesarul de Căldură de Calcul. Prescripții de Calcul (Heating Installations. Calculation Heat Requirement. Calculation Prescriptions). Institutul Român de Standardizare (Romanian Institut of Standardization): București, Romania, 1997.
34. I.R.S. SR 1907-2:1997; Instalatii de Incalzire. Necesarul de Căldură de Calcul. Temperaturi Interioare Convenționale de Calcul (Heating Installations. Calculation Heat Requirement. Conventional Interior Temperatures for Calculation). Institutul Român de Standardizare (Romanian Institut of Standardization): București, Romania, 1997.
35. URBAN-INCERC C 107/1-2005; Normativ Privind Calculul Coeficienților Globali de Izolare Termică La Clădirile de Locuit (Normative Regarding the Calculation of Global Coefficients of Thermal Insulation for Residential Buildings). Fast Print: București, Romania, 2005. Available online: <https://www.star.ugal.ro/crios/Support/IEACA/Anexe/C107-1-3-2005.pdf> (accessed on 23 June 2023).
36. ASRO SR 4839; Instalații de Încălzire Numărul Anual de Grade-Zile (Heating Systems Annual Number of Degree-Days); Asociația de Standardizare din România (Romanian Standardization Association): București, Romania, 2014.
37. GeoT*SOL | Calculation and Simulation Software for Heat Pump Systems. Available online: <https://valentin-software.com/en/products/geotsol/> (accessed on 23 June 2023).
38. GeoT*SOL® Exploiting the Earth's Sustainable Energy Supply Planning Programs from Valentin Software. Available online: <https://solsta.co/uploads/product/4a960ac291a543828795731231fb56a0/datasheet-geot-sol.pdf> (accessed on 24 June 2023).
39. Solar Resource Maps and GIS Data for 200+ Countries | Solargis. Available online: <https://solargis.com/maps-and-gis-data/download/romania> (accessed on 20 June 2023).
40. ASTM Standard C 168-97; Terminology Relating to Thermal Insulating Materials. ASTM International: West Conshohocken, PA, USA, 1997.
41. ASHRAE HANDBOOK 2001 Fundamentals; American Society of Heating, Refrigerating and Air-Conditioning Engineers: Atlanta, GA, USA, 2001.
42. Al-Homoud, M.S. Performance Characteristics and Practical Applications of Common Building Thermal Insulation Materials. *Build. Environ.* **2005**, *40*, 353–366. [[CrossRef](#)]
43. Zhou, X.-Y.; Zheng, F.; Li, H.-G.; Lu, C.-L. An Environment-Friendly Thermal Insulation Material from Cotton Stalk Fibers. *Energy Build.* **2010**, *42*, 1070–1074. [[CrossRef](#)]
44. Kumar, D.; Alam, M.; Zou, P.X.W.; Sanjayan, J.G.; Memon, R.A. Comparative Analysis of Building Insulation Material Properties and Performance. *Renew. Sustain. Energy Rev.* **2020**, *131*, 110038. [[CrossRef](#)]
45. Cuce, E.; Cuce, M.; Wood, C.J.; Riffat, S.B. Toward Aerogel Based Thermal Superinsulation in Buildings: A Comprehensive Review. *Renew. Sustain. Energy Rev.* **2014**, *34*, 273–299. [[CrossRef](#)]
46. Bjørn, P.J. Traditional, State-of-the-Art and Future Thermal Building Insulation Materials and Solutions-Properties, Requirements and Possibilities. *Energy Build.* **2011**, *43*, 2549–2563. [[CrossRef](#)]
47. Johnson, N.A.G.; Wood, E.J.; Ingham, P.E.; McNeil, S.J.; McFarlane, I.D. Wool as a Technical Fibre. *J. Text. Inst.* **2009**, *94*, 26–41. [[CrossRef](#)]
48. Ye, Z.; Wells, C.M.; Carrington, C.G.; Hewitt, N.J. Thermal Conductivity of Wool and Wool-Hemp Insulation. *Int. J. Energy Res.* **2006**, *30*, 37–49. [[CrossRef](#)]
49. Zach, J.; Korjenic, A.; Petráněk, V.; Hroudová, J.; Bednar, T. Performance Evaluation and Research of Alternative Thermal Insulations Based on Sheep Wool. *Energy Build.* **2012**, *49*, 246–253. [[CrossRef](#)]
50. Czajkowski, Ł.; Wojcieszak, D.; Olek, W.; Przybył, J. Thermal Properties of Fractions of Corn Stover. *Therm. Prop. Fractions Corn Stover* **2019**, *210*, 709–712. [[CrossRef](#)]
51. Brzyski, P.; Barnat-Hunek, D.; Suchorab, Z.; Łagód, G. Composite Materials Based on Hemp and Flax for Low-Energy Buildings. *Materials* **2017**, *10*, 510. [[CrossRef](#)]
52. Lekavicius, V.; Shipkovs, P.; Ivanovs, S.; Rucins, A. Thermo-Insulation Properties of Hemp-Based Products. *Latv. J. Phys. Tech. Sci.* **2015**, *52*, 38–51. [[CrossRef](#)]
53. Barrau, J.; Ibanez, M.; Badia, F. Impact of the Insulation Materials' Features on the Determination of Optimum Insulation Thickness. *Int. J. Energy Environ. Eng.* **2014**, *5*, 79. [[CrossRef](#)]
54. Tuzcu, T.M. Hygro-Thermal Properties of Sheep Wool Insulation. Master's Thesis. Available online: <https://repository.tudelft.nl/islandora/object/uuid%3A6f32b195-f2b7-41e4-b70e-adae72c078e9> (accessed on 26 June 2023).
55. Hossain, A.; Mourshed, M. Retrofitting Buildings: Embodied & Operational Energy Use in English Housing Stock. *Proceedings* **2018**, *2*, 1135. [[CrossRef](#)]

56. Memon, S. Analysing the Potential of Retrofitting Ultra-Low Heat Loss Triple Vacuum Glazed Windows to an Existing UK Solid Wall Dwelling. *Int. J. Renew. Energy Dev.* **2014**, *3*, 161–174. [[CrossRef](#)]
57. Wang, X.; Xia, L.; Bales, C.; Zhang, X.; Copertaro, B.; Pan, S.; Wu, J. A Systematic Review of Recent Air Source Heat Pump (ASHP) Systems Assisted by Solar Thermal, Photovoltaic and Photovoltaic/Thermal Sources. *Renew. Energy* **2019**, *146*, 2472–2487. [[CrossRef](#)]
58. Menegazzo, D.; Lombardo, G.; Bobbo, S.; De Carli, M.; Fedele, L. State of the Art, Perspective and Obstacles of Ground-Source Heat Pump Technology in the European Building Sector: A Review. *Energies* **2022**, *15*, 2685. [[CrossRef](#)]
59. Badiel, A.; Akhlaghi, Y.G.; Zhao, X.; Shittu, S.; Xiao, X.; Li, J.; Fan, Y.; Li, G. A Chronological Review of Advances in Solar Assisted Heat Pump Technology in 21st Century. *Renew. Sustain. Energy Rev.* **2020**, *132*, 132. [[CrossRef](#)]
60. Popescu, R. *St. Utilizarea Energiei Regenerabile În Clădiri (Use of Renewable Energy in Buildings)*; Matrix Rom: București, Rumania, 2016.
61. Catalina, T. *Utilizarea Surselor de Energie Regenerabilă În Clădiri (The Use of Renewable Energy in Buildings)*; Matrix Rom: București, Rumania, 2015.
62. Abdelaal, A.K.; El-Fergany, A. Estimation of Optimal Tilt Angles for Photovoltaic Panels in Egypt with Experimental Verifications. *Sci. Rep.* **2023**, *13*, 3268. [[CrossRef](#)]
63. Tokar, D.; Muntean, D.; Tokar, A. Aspecte privind influența umbririi panourilor fotovoltaice asupra producției de energie electrică. Studiu de caz. (Aspects regarding the influence of shading photovoltaic panels on electricity production. Case study). *Revista Ingineria Instalațiilor (Building Services Engineering Magazine)*, No. II/2023, 6 July 2023; pp. 30–36.
64. Energy Consumption in Households—Statistics Explained. Available online: https://ec.europa.eu/eurostat/statistics-explained/index.php?title=Energy_consumption_in_households#Energy_consumption_in_households_by_type_of_end-use (accessed on 22 June 2023).
65. Statistics | Eurostat. Available online: https://ec.europa.eu/eurostat/databrowser/explore/all/envir?lang=en&subtheme=nrg.nrg_quant.nrg_quanta&display=list&sort=category (accessed on 22 June 2023).
66. The REPowerEU Plan Explained—Consilium. Available online: <https://www.consilium.europa.eu/en/infographics/repowereu/> (accessed on 22 June 2023).
67. McKinsey: Banks Could Lend EUR 20 Bln to Finance Romania’s Green Transition | Romania Insider. Available online: <https://www.romania-insider.com/mckinsey-banks-loans-romania-green-transition-2023> (accessed on 22 June 2023).
68. Electricity & Gas Hit Record Prices in 2022—Products Eurostat News—Eurostat. Available online: <https://ec.europa.eu/eurostat/web/products-eurostat-news/w/DDN-20230426-2> (accessed on 20 June 2023).
69. Mohammed, G.A.; Mabrouk, M.; He, G.; Abdrabo, K.I. Towards Sustainable Cities: A Review of Zero Energy Buildings Techniques and Global Activities in Residential Buildings. *Energies* **2023**, *16*, 3775. [[CrossRef](#)]
70. Bellos, E.; Tzivanidis, C.; Moschos, K.; Antonopoulos, K.A. Energetic and Financial Evaluation of Solar Assisted Heat Pump Space Heating Systems. *Energy Convers. Manag.* **2016**, *120*, 306–319. [[CrossRef](#)]
71. Zhang, S.; Ocloń, P.; Klemeš, J.J.; Michorczyk, P.; Pielichowska, K.; Pielichowski, K. Renewable Energy Systems for Building Heating, Cooling and Electricity Production with Thermal Energy Storage. *Renew. Sustain. Energy Rev.* **2022**, *165*, 2560. [[CrossRef](#)]

Disclaimer/Publisher’s Note: The statements, opinions and data contained in all publications are solely those of the individual author(s) and contributor(s) and not of MDPI and/or the editor(s). MDPI and/or the editor(s) disclaim responsibility for any injury to people or property resulting from any ideas, methods, instructions or products referred to in the content.